



Defence Research and  
Development Canada

Recherche et développement  
pour la défense Canada



# **A comparative analysis of computed and measured SAR images of complex targets**

S. Wong, N. Sandirasegaram, R. English, C. Liu, P. Vachon and J. Wolfe

**Defence R&D Canada – Ottawa**

Technical Memorandum  
DRDC Ottawa TM 2012-016  
May 2012

**Canada**



# **A comparative analysis of computed and measured SAR images of complex targets**

S. Wong, N. Sandirasegaram, R. English, C. Liu, P. Vachon and J. Wolfe

**Defence R&D Canada – Ottawa**

Technical Memorandum

DRDC Ottawa TM 2012-016

May 2012

Principal Author

*Original signed by S. Wong*

---

S. Wong  
Defence Scientist

Approved by

*Original signed by C. Wilcox*

---

C. Wilcox  
Section Head/RAST

Approved for release by

*Original signed by C. McMillan*

---

C. McMillan  
Chief Scientist

## Abstract

---

Computational radar target signature generation is considered as an integral component of a future target recognition system. It provides a comprehensive reference library database for target identification of a wide variety of targets, for example, aircraft, marine vessels and ground vehicles. Compiling an operational library will require an electromagnetic code that is capable of generating reliable and robust radar target signatures. Presently, computational electromagnetic modelling technology is not sufficiently mature to provide such a capability. To assess the quality of the computed target signatures from what is available with current technology, SAR (Synthetic Aperture Radar) images of complex targets generated by electromagnetic modelling computation are compared against measured SAR data of real targets.

An armoured personnel carrier, a self-propelled howitzer, a naval warship and a sea-going ferry are used as targets in the investigation. The commercial electromagnetic modelling code FACETS (Frequency Asymptotic Code for Electromagnetic Target Scattering) is used for generating the SAR images. CAD (Computer-Aided Design) models of targets of interest are used as inputs to the modelling code. Measured SAR images of corresponding targets from the MSTAR (Moving and Stationary Target Acquisition and Recognition) public release datasets and from the RadarSat2 SAR imagery archive are used to compare against the computed images. The objective is to analyze and characterize the computed image of complex targets; this facilitates a better understanding of the computational target signature generation problem.

## Résumé

---

On considère que la génération computationnelle de signatures de cibles radar est un élément essentiel aux futurs systèmes de reconnaissance des cibles. Cette technologie fournit une base de données de référence complète pour l'identification d'une grande variété de cibles, comme les avions, les navires et les véhicules terrestres. La compilation d'une bibliothèque opérationnelle nécessite un code électromagnétique qui peut générer des signatures de cibles radar fiables et robustes. Présentement, la technologie de la modélisation électromagnétique computationnelle n'est pas suffisamment avancée pour offrir une telle capacité. Afin d'évaluer la qualité des signatures de cibles calculées à l'aide de la technologie présentement disponible, on a procédé à la comparaison entre des images de radar à synthèse d'ouverture (SAR) de cibles complexes générées par modélisation électromagnétique computationnelle et des cibles réelles de données SAR mesurées.

Dans le cadre de la présente recherche, on a utilisé comme cibles un véhicule blindé de transport de troupes, un obusier automoteur, un navire de guerre et un traversier océanique. On a utilisé le code de modélisation électromagnétique computationnel commercial FACETS (code de fréquence asymptotique pour la diffusion de cibles électromagnétiques) pour générer les images SAR. On a utilisé comme intrants au code de modélisation des modèles de conception assistée par ordinateur (CAO) des cibles concernées. On a utilisé des images SAR mesurées des cibles correspondantes provenant des ensembles de données pour diffusion publique MSTAR

(acquisition et reconnaissance de cibles mobiles et fixes) et des archives d'images SAR du RADARSAT-2 pour les comparer aux images calculées. L'objectif consiste à analyser et à caractériser les images calculées de cibles complexes afin de mieux comprendre les problèmes reliés à la génération computationnelle de signatures de cibles radar.

## Executive summary

---

### A comparative analysis of computed and measured SAR images of complex targets

S. Wong, N. Sandirasegaram, R. English, C. Liu, P. Vachon and J. Wolfe; DRDC Ottawa TM 2012-016; Defence R&D Canada – Ottawa; May 2012.

**Introduction or background:** A comparative analysis is conducted to assess the capability of the electromagnetic modelling technology for generating a synthetic target image database for target recognition and verification applications. It is generally agreed that the current electromagnetic modelling technology is not yet mature enough to provide reliable and robust synthetic radar target images for performing machine-based target recognition automatically. However, it may be useful as a tool to assist human analysts to determine the target type in a verification process for AIS (Automatic Identification System) and IFF (Identification Friend or Foe) applications.

Target verification is an integral part of a target recognition system. It is known that cooperative identification methods such as AIS and IFF can be subjected to spoofing. Thus, an independent means to confirm the identity of a target of interest is imperative. Radar images of an interrogated target can be used to support the verification process. Radar images are applicable day or night, and under all-weather conditions.

In the target verification process, a library database of radar target images is required as reference to compare with the captured image of an interrogated target. Compiling a library database by measurements is impractical and very expensive. Firstly, accessing targets of interest for imaging would be very difficult, if not impossible. Secondly, the cost of acquiring and maintaining a radar facility for target image measurement would be prohibitive. Thirdly, conducting measurement trials can also be very costly and time consuming. Generating target images synthetically is seen as a viable solution to the library database problem, especially when a large number of target types and hostile targets are sought.

Currently, electromagnetic modelling technology for generating radar target signatures is still considered as being in the developmental stage. It is not yet mature enough to be able to generate high fidelity radar images of complex targets. But the level of fidelity may be adequate enough such that the computed images are useful as reference aids to human analysts for identifying or verifying targets.

DRDC Ottawa has a functional electromagnetic modelling capability to generate radar images of complex targets such as aircraft, ships and ground vehicles. Radar images are computed using the electromagnetic modelling code, FACETS (Frequency Asymptotic Code for Electromagnetic Target Scattering). The FACETS code has been validated using a canonical target that is composed of basic scattering primitives.

In this report, Synthetic Aperture Radar (SAR) images of an armoured personnel carrier, a self-propelled howitzer, a naval warship and a catamaran ferry are computed and compared against measured radar image data. The comparative analysis provides an assessment on the quality of the computed radar images.

**Results:** Results in this study have indicated that generating robust and high-fidelity target images by computational modelling remains a challenge. Some of the problems concerning the generation of good quality images are identified. Prospective applications using images of limited quality for human-assisted target identification/verification are discussed.

**Significance:** Although the quality of the computed target images of complex targets are still not reliable enough to be used for machine-based automatic target identification, the general target profiles of the computed target images contain relevant distinct features; these can be exploited by human analysts in ISR (Intelligence, Surveillance and Reconnaissance) applications.

**Future plans:** An on-going in-depth evaluation of the computed images of an ocean-going ferry is presently being carried out by comparing the computed images against very high resolution measured SAR images. The use of very high resolution, about 0.15m, permits distinct features at particular locations on the target to be examined in greater detail. Some of these specific sites have corresponding basic scattering primitive shapes that are useful for characterizing the image computational process. A better understanding of the computational electromagnetic modelling problem would offer greater insights into how the fidelity of the computed target images can be improved.

The electromagnetic modelling work presented in this work is currently being applied to support target characterization studies of marine targets (commercial ships) and small land targets (trucks) in collaborative projects with external research partners, e.g., NATO task groups. These studies will help to further develop the computational target signature capability for exploiting SAR imagery to extract target identification information. A collaborative project will be proposed to the CF Joint Imagery Centre to explore SAR image analysis techniques for finding and identifying various types of targets of interests, for example, ballistic missile launching platforms, ships and aircraft that are present at strategic locations of interest. The objective of the project is to help the CF to explore and develop enhanced capability for retrieving relevant target information from SAR imagery data in support of mission planning, allowing the CF to be more effective in conducting their operations.

## Sommaire

---

### **A comparative analysis of computed and measured SAR images of complex targets**

**S. Wong, N. Sandirasegaram, R. English, C. Liu, P. Vachon and J. Wolfe; DRDC Ottawa TM 2012-016; R & D pour la défense Canada – Ottawa; Mai 2012.**

**Introduction ou contexte:** On a procédé à une analyse comparative afin d'évaluer la capacité de la technologie de modélisation électromagnétique à générer une base de données d'images synthétiques de cibles pour des applications de reconnaissance et de vérification des cibles. Il est généralement admis que la technologie de modélisation électromagnétique actuelle n'est pas suffisamment avancée pour produire des images synthétiques de cibles radar assez fiables et robustes pour permettre la reconnaissance automatique de cibles par des machines. Toutefois, cette technologie peut être utile comme outil pour aider les analystes humains à déterminer le type de cibles dans le cadre d'applications d'un processus de vérification d'un système d'identification automatique (SIA) et d'un système d'identification ami/ennemi (IFF).

La vérification des cibles est une partie intégrante de tout système de reconnaissance des cibles. On sait qu'il est possible de mystifier les méthodes d'identification coopératives comme le SIA et l'IFF. Par conséquent, il est impératif de pouvoir confirmer l'identité d'une cible d'intérêt à l'aide d'un moyen indépendant. On peut utiliser les images radar d'une cible interrogée pour appuyer le processus de vérification. Les images radar sont utilisables de jour comme de nuit et dans toutes les conditions météorologiques.

Dans le processus de vérification des cibles, il faut recourir à une base de données de référence des images de cibles radar pour fins de comparaison avec l'image capturée de la cible interrogée. La compilation d'une base de données de référence à partir de mesures n'est pas pratique et est très dispendieuse. Premièrement, il serait très difficile, voire impossible, d'avoir accès aux cibles d'intérêt à des fins de formation d'images. Deuxièmement, il serait prohibitif de faire l'acquisition et l'entretien d'une installation radar dans le seul but de prendre des mesures des cibles à des fins d'imagerie. Troisièmement, les essais visant à procéder à des mesures peuvent prendre beaucoup de temps et être également très coûteux. La génération d'images synthétiques de cibles est considérée comme une solution viable au problème de base de données de référence, surtout lorsqu'il est question de traiter un grand nombre de types de cibles et des cibles hostiles.

Présentement, on considère que la technologie de la modélisation électromagnétique appliquée à la génération de signatures de cibles radar est encore au stade expérimental et qu'elle n'est pas encore assez avancée pour pouvoir générer des images radar à haute fidélité de cibles complexes. Toutefois, le niveau de fidélité actuel peut être suffisant pour que les images calculées soient utiles aux analystes humains pour l'identification ou la vérification de cibles.

Le RDDC Ottawa possède une capacité de modélisation électromagnétique fonctionnelle permettant de générer des images radar de cibles complexes comme des aéronefs, des navires et des véhicules terrestres. Les images radar sont calculées à l'aide du code de modélisation électromagnétique FACETS (code de fréquence asymptotique pour la diffusion de cibles

électromagnétiques). Le code FACETS a été validé à l'aide d'une cible de type canonique composée de primitives de diffusion de base.

Dans le présent rapport, les images de radar à synthèse d'ouverture (SAR) d'un véhicule blindé de transport de troupes, d'un obusier automoteur, d'un navire de guerre et d'un traversier catamaran sont calculées et comparées aux données des images radar mesurées. L'analyse comparative fournit une évaluation de la qualité des images radar calculées.

**Résultats:** Les résultats de la présente étude révèlent qu'il est encore difficile de générer des images de cibles à haute fidélité et robustes à l'aide d'une modélisation computationnelle. Le rapport identifie certains des problèmes associés à la génération d'images de bonne qualité. Le rapport traite également des applications potentielles de l'utilisation d'images de qualité limitée pour les opérations d'identification et de vérification de cibles avec intervention humaine.

**Importance:** Même si la qualité des images de cibles complexes calculées n'est pas encore suffisamment fiable pour permettre l'identification automatique de cibles par des machines, les profils généraux des images de cibles calculées contiennent néanmoins des caractéristiques distinctes susceptibles d'être exploitées par des analystes humains pour des applications liées à des missions de renseignement, de surveillance et de reconnaissance (RSR).

**Perspectives:** On poursuit actuellement l'évaluation approfondie des images calculées d'un traversier océanique comparativement à des images SAR mesurées à très haute résolution. L'utilisation de la très haute résolution, environ 0,15 m, permet d'examiner de façon détaillée des caractéristiques distinctes situées à des endroits particuliers sur la cible. Certains de ces sites spécifiques présentent des formes primitives de diffusion de base correspondantes qui sont utiles pour la caractérisation du processus computationnel de l'image. Une meilleure compréhension des problèmes liés à la modélisation électromagnétique computationnelle permettrait de trouver des façons d'améliorer la fidélité des images de cibles calculées.

Les activités de modélisation électromagnétique présentées dans le présent document sont actuellement appliquées pour faciliter les études de caractérisation de cibles marines (navires commerciaux) et de petites cibles terrestres (camions) dans le cadre de projets de collaboration avec des partenaires de recherche externes, comme des groupes de travail de l'OTAN. Ces études aideront à poursuivre le développement de la capacité computationnelle des signatures de cibles pour exploiter l'imagerie SAR afin d'extraire des informations relatives à l'identification de cibles. Un projet de collaboration sera proposé au Centre d'imagerie interarmées des Forces canadiennes en vue d'étudier les techniques d'analyse d'images SAR afin de trouver et de déterminer divers types de cibles d'intérêt, comme des plates-formes de lancement de missiles balistiques, des navires et des avions situés aux emplacements stratégiques d'intérêt. Le projet vise à aider les FC à étudier et à développer une capacité accrue de récupération des informations pertinentes sur les cibles à partir des données d'images SAR à l'appui de la planification de missions, et ainsi permettre aux FC d'améliorer leur efficacité lors de la conduite d'opérations.

# Table of contents

---

Abstract .....	i
Résumé .....	i
Executive summary .....	iii
Sommaire .....	v
Table of contents .....	vii
List of figures .....	viii
List of tables .....	x
Acknowledgements .....	xi
1 Introduction.....	1
2 Synthetic SAR Image Generation Tools.....	2
2.1 A description of the FACETS code.....	2
2.2 Target CAD (computer-Aided Design) Models .....	3
3 Measured Target SAR Images .....	6
3.1 MSTAR Datasets.....	6
3.2 RADARSAT2 Data .....	6
4 Comparisons between measured and computed SAR images .....	7
4.1 BTR70, armoured personnel carrier .....	7
4.2 Gvozdika, self-propelled howitzer .....	12
4.3 Naval warships .....	21
4.4 “Alboran”, a catamaran ferry.....	25
5 Conclusions.....	29
References .....	31

## List of figures

---

Figure 1: Examples of various basic scattering primitives to illustrate single, double, triple and multiple-bounce processes.....	2
Figure 2: Photo and CAD model of the BTR70 armoured personnel carrier.....	4
Figure 3: Photo and CAD model of the Gvozdika self-propelled howitzer.....	4
Figure 4: Photos of the catamaran ferry, “HSC Alboran”, showing the actual configuration.....	4
Figure 5: CAD model of the catamaran ferry HCS Alboran; top: original model, bottom: modified model with added cabin to the back of the rear deck.....	5
Figure 6: comparisons between measured and computed SAR images of the BTR70.....	9
Figure 7: Comparisons between measured and computed SAR images near head-on aspect viewing angles.....	11
Figure 8: CAD model of engine compartment hatch doors.....	12
Figure 9: Gvozdika’s track-and-wheel drive.....	12
Figure 10: Comparison between measured and computed SAR images of the Gvozdika.....	13
Figure 11: Comparisons between measured and computed images at head-on aspects.....	16
Figure 12: Photo of the exhaust manifolds on a Gvozdika (top), CAD model of the exhaust manifolds (bottom).....	17
Figure 13: Comparisons between measured and computed images of the Gvozdika at tail-on aspect.....	18
Figure 14: Photo of the headlight cover on the Gvozdika (top), CAD model (bottom).....	19
Figure 15: Comparisons between measured and computed images of a canonical target [11]. ....	20
Figure 16: Comparison between measured image (a) and computed image (b) of a naval vessel using a high-precision CAD model. Incidence angle = 30.5 deg., azimuth = -5.9 deg.....	21
Figure 17: Comparison between measured image (a) and computed image (b) of a naval vessel using a high-precision CAD model. Incidence angle = 30.5 deg., azimuth = -8.4 deg.....	22
Figure 18: Comparison between measured image (a) and computed image (b) using a commercial CAD model. Incidence angel = 30.5 deg., azimuth angle = -5.9 deg.....	23
Figure 19: Dihedral structure formed at the bridge location of the vessel; top: high-precision CAD model, bottom: commercial CAD model.....	24
Figure 20: Comparisons of the bridge dihedral structure scattering behaviour between the high-precision CAD model and the commercial CAD model at different azimuth angles; the negative sign indicates viewing the starboard side.....	25
Figure 21: Two measured SAR images of the catamaran ferry, “Alboran”; image captured at: a) incidence angle = 48.4 deg, b) incidence angle = 34 deg.....	26

Figure 22: Optical views of 2 possible orientations of the SAR images of the docked ferry in Figure 21a; a) azimuth = 152 deg., b) azimuth = -28 deg. .... 27

Figure 23: Comparison between the measured image (a) and the computed image (b) of the ferry. Computed image: incidence angle = 48.4 deg., azimuth angle = -28 deg (viewed from the front of the ferry). .... 27

Figure 24: Comparison between the measured image (a) and the computed image (b) of the ferry. Computed image: incidence angle = 48.4 deg., azimuth angle = 152 deg (viewed from the back of the ferry). .... 28

Figure 25: Comparison between the measured image (a) and the computed image (b) of the ferry. .... 28

## List of tables

---

Table 1: Cross-correlation scores as a function of azimuth angle for the BTR70.....	7
Table 2: Cross-correlation scores as a function of azimuth angles for the Gvozdika. ....	15

## **Acknowledgements**

---

The authors would like to acknowledge Mr. Simon Carbonneau of nEW Technologies for his diligence and excellent work in preparing the CAD models of some very complex targets for computation in the electromagnetic modelling code.

This page intentionally left blank.

# 1 Introduction

---

In a target identification/verification system, a reference library database containing a set of target signatures, such as SAR images, of different target types is required to assist the identification process. Compiling a functional database for an operational system is a major challenge. There are still many technical issues to be resolved before a practical database can be realized. Compiling a useful database by real measurements is seen as impractical. Target signature generation by computational methods is regarded as a viable alternative [1]. There has been a considerable amount of research activities carried out in the area of synthetic target signature generation within the defence research community.

The generation of target signatures involves the use of computational electromagnetic modelling (CEM) codes, and computer-aided design (CAD) models of targets of interests. CEM codes can simulate radar scattering processes of complex targets such as aircraft, ships and vehicles. CAD models provide the geometrical descriptions of the targets to the CEM codes to compute the scattering processes. The computed target signatures can be in the form of high range resolution profiles (1-D image), SAR images (2-D), or 3-D target images [2]. The CEM technology is not yet mature. Computed target signatures are not considered as robust and reliable enough to be useful in an operational environment. Validation of the CEM process is a necessary step before practical applications can be realized; validation has been a topic of interest within the electromagnetic community [3][4]. To evaluate the modelling techniques and algorithmic codes, it is a common practice to gain acceptance and confidence by comparing the computed results against measurements [5][6][7]. Trying to achieve computation-to-measurement validation within a consistent level of accuracy has been a challenge and is still an on-going endeavour in CEM research.

In this report, an evaluation on the quality of the computed SAR images of a number of different target types is conducted. A commercial CEM code and commercial CAD models of targets of interests are used in the evaluation. The computed SAR images are compared with available measured data of real targets to assess the image fidelity. Two land vehicles and two marine vessels, are examined. The objective is to obtain a better understanding of the computational outputs from the CEM code, and to gain some insights on how the fidelity of the computed images can be improved.

## 2 Synthetic SAR Image Generation Tools

---

### 2.1 A description of the FACETS code

The FACETS (Frequency Asymptotic Code for Electromagnetic Target Scattering) code is a commercial CEM product developed by Thales Defence Information Systems, UK. FACETS is capable of computing radar cross sections and SAR images of complex targets; it employs a combination of physical optics and geometrical optics to model basic scattering processes such as single-bounce, double-bounce (dihedral) and triple-bounce (trihedral) reflections from the surfaces of a target [8]. FACETS is also capable of computing scattering from duct and cavities using multiple-bounce ray tracing technique. In essence, FACETS decomposes a complex target into different types of scattering primitive; these scattering primitives are illustrated in Figure 1. Edge scattering from a target is handled using various diffraction methods such as curved surface diffraction, reflection diffraction, edge travelling wave and surface creeping wave. Although diffraction is largely a second order effect comparing to the double-bounce and triple-bounce scattering processes, it may contribute considerably to the target image under some circumstances.

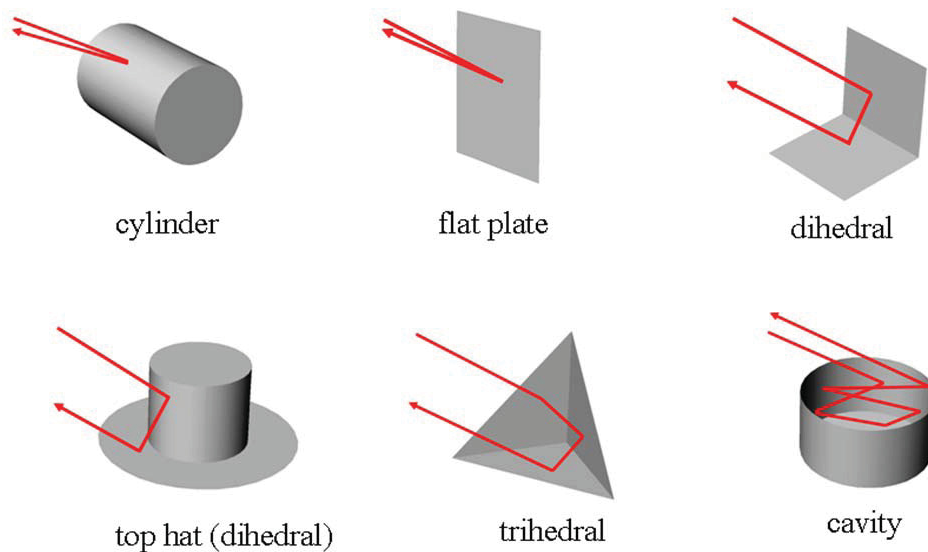


*Figure 1: Examples of various basic scattering primitives to illustrate single, double, triple and multiple-bounce processes.*

FACETS has the capability to compute the SAR image of a target that has different surface material types: perfect electric conducting, dielectric and radar absorbing materials. FACETS can also provide a range of computational options, for example, mono-static, bi-static, near-field and far-field scattering. Furthermore, one-dimensional High range resolution profiles and 2-dimensional SAR images can be computed simultaneously. Computations of the four polarizations, HH, VV, HV and VH are done simultaneously, generating fully polarimetric radar images.

Target geometry information required by FACETS is provided by a CAD model of the target of interest. FACETS accepts only geometry given by the mathematical representation known as Parametric Bi-Cubic surfaces. Conventionally, curved surfaces in a CAD model are given by the NURBS (Non-Uniform Rational B-Splines) format. A NURBS surface is represented by a number of piece-wise polynomial fitting curves to provide a smooth geometrical fit to the target's shape. In order for FACETS to utilize the target's shape information for computation, the CAD model must be converted from NURBS format to Parametric Bi-Cubic format. The CAD software tool, PATRAN is used for the format conversion of the CAD models. Other input parameters required for image computation are the radar frequency, radar bandwidth, angular aperture size and target aspects (elevation and azimuth angles).

FACETS employs a modular structure for computing various scattering processes. It has a single-bounce scattering algorithm that computes the basic scattering from surfaces such as flat plates, cylinders and spheres. In computing more complex processes such as double-bounce, triple-bounce and multiple-bounce scattering, FACETS has recognized that it would be difficult to determine and apply accurately the appropriate algorithms to compute these processes in an automatic manner. Thus, FACETS requires these scattering processes to be specified manually as inputs for computation; that is, the locations and the types of scattering process on the target CAD model must be identified by a human operator manually. For real-world complex targets such as aircraft, ground vehicles and ships, the nomination of the appropriate scattering processes can be quite labour intensive.

## **2.2 Target CAD (Computer-Aided Design) Models**

Two ground vehicles and two marine vessels are investigated in this study. The CAD models for these targets are obtained from commercial sources. Commercial CAD models can be described as having good resemblance to the real targets visually; they are not expected to be accurate in the physical details in terms of the target geometry and dimensions. In fact, the physical dimensions of a couple of the CAD models used in this investigation have to be rescaled in their length, width and height to conform to those of the standard version of the real targets.

There is a degree of uncertainty in the accuracy of these CAD models in representing the actual measured targets because of a lack of information on specific physical details of the actual measured targets; only photographs of the typical target types are available as reference. Figure 2 and Figure 3 show the CAD models and sample picture of the two ground vehicles, an armoured personnel vehicle (BTR70) and a self-propelled howitzer (Gvozdika) respectively. The CAD models can only be said to provide a general overall geometrical description of the targets in appearance. A naval warship is examined as one of the two marine vessels. The CAD models of the warship will not be shown or described here in order to comply with the unclassified designation of this document. The second marine vessel investigated is a catamaran ferry. A picture of the ferry, "HSC Alboran" is shown in Figure 4. The "Alboran" is chosen because measured SAR images of this specific ferry are available. The CAD model of the ferry is modified to match the physical configuration of the "Alboran". An extra covered section is added to the rear deck section of the ferry. Illustrations of the original CAD model and the modified CAD model of the ferry are shown in Figure 5.

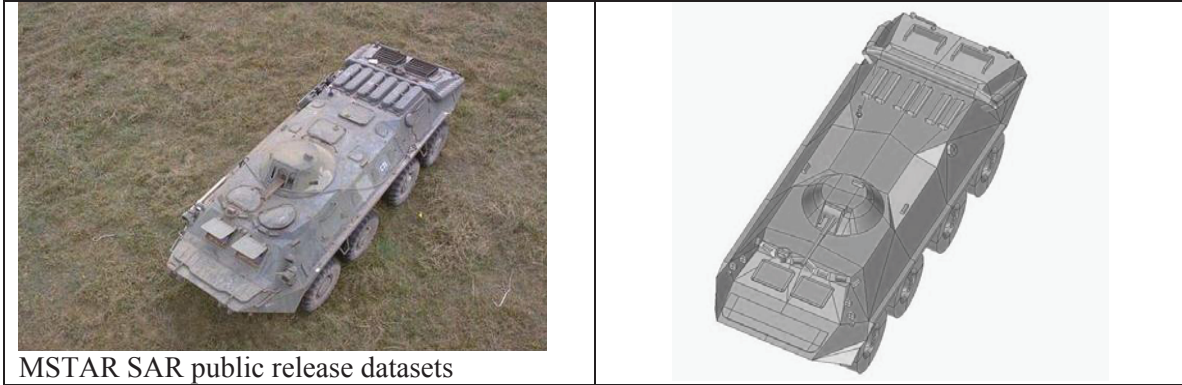


Figure 2: Photo and CAD model of the BTR70 armoured personnel carrier.

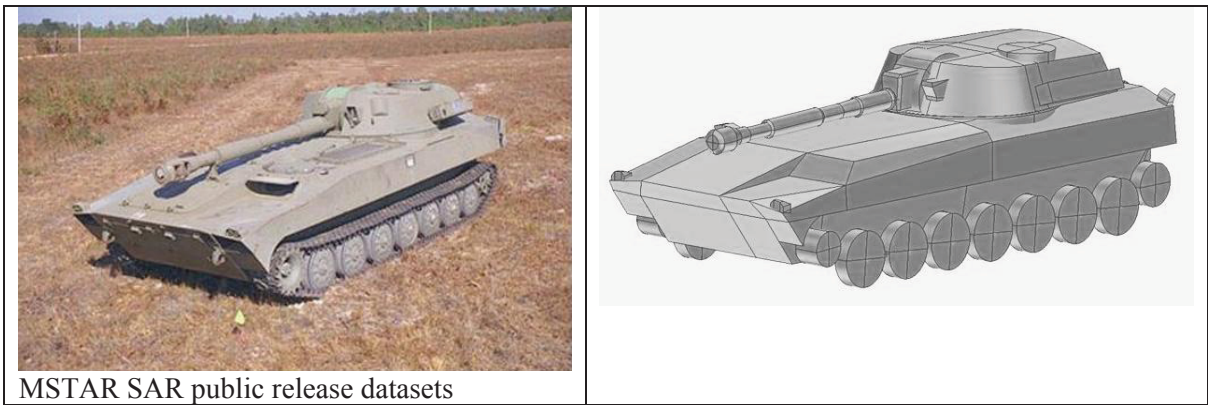
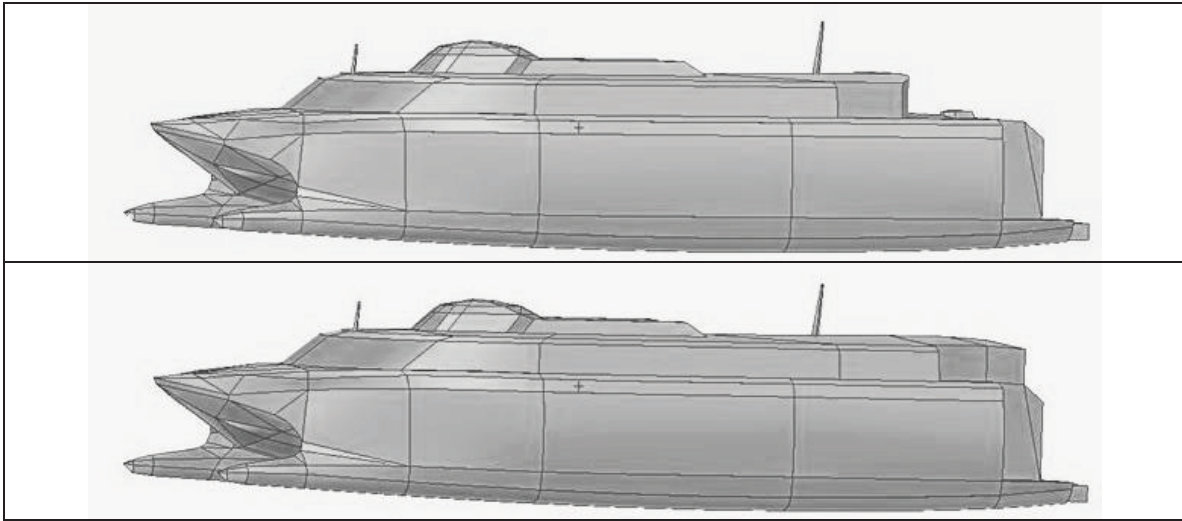


Figure 3: Photo and CAD model of the Gvozdika self-propelled howitzer.



Figure 4: Photos of the catamaran ferry, “HSC Alboran”, showing the actual configuration.



*Figure 5: CAD model of the catamaran ferry HCS Alboran; top: original model, bottom: modified model with added cabin to the back of the rear deck.*

## **3 Measured Target SAR Images**

---

### **3.1 MSTAR Datasets**

The MSTAR (Moving and Stationary Target Acquisition and Recognition) Public Release Datasets contain measured SAR images of a number of military ground vehicles. The BTR70 and the Gvozdika are two of the targets in the MSTAR datasets. SAR images were collected from an air-borne radar system using the spotlight mode at a radar frequency of 9.6 GHz. The SAR images were taken from 0 to 360 degrees in azimuth, and at a depression (elevation) angle of 15 degrees. The spotlight SAR radar was flown several times around the targets, providing multiple 360-degree azimuth coverage. Accurate ground truth data for the SAR images are available. The images were captured with equal down-range and cross-range resolutions of 0.3m. But the data were processed to give effective down-range and cross-range pixel spacing of 0.2m.

### **3.2 RADARSAT2 Data**

Measured SAR images of two naval warships of the same vessel type and a catamaran ferry are available in the RADARSAT2 SAR imagery archive. For the warships, the images were captured in spotlight mode at a radar frequency of 5.4 GHz and an incidence angle of 30.5 degrees with respect to the vertical. The image resolutions are 1.6m and 0.8m in the range and azimuth direction respectively. The processed SAR image data are given with a pixel spacing of 1.33m (range) and a line spacing of 0.35m (azimuth).

For the catamaran ferry, the SAR images were captured in ultra-fine, strip-map mode at 5.4 GHz. The image resolutions are 1.6m and 2.8m in range and azimuth respectively. The processed data are given with pixel spacing of 1.33m (range), and 2.04m (azimuth). Measured images of the docked ferry are available at two different viewing aspects (incidence and azimuth angles).

## 4 Comparisons between measured and computed SAR images

---

### 4.1 BTR70, armoured personnel carrier

In the computation of the BTR70, the vehicle's body is assumed to be metallic (i.e., highly radar reflective), and the tires are non-reflective. The computed images are generated by treating the target's CAD model as an isolated object; that is, there is no ground-plane interaction included in the computation. Although the actual measured target was placed in an open field where ground interaction is expected, a previous analysis using another target from the MSTAR datasets has indicated that the ground interaction effect is minimal on the measured images and it has no effect in the comparative analysis between the computed and measured images [9].

A comparison between the computed and measured images of the BTR70 is shown in Figure 6; the images are sampled at a 45-degree interval covering 360 degrees in azimuth. It can be seen that at some viewing angles, the images are matching reasonably well; at other angles, the agreements in the comparison are poor. The best matches are at head-on (0 azimuth) and the broad-side (90 and 270-degree azimuth) angles from visual inspection. Many of the scatterers that appear in the measured images also appear in the computed images at these azimuth viewing angles. At 45-degree viewing angles with respect to the target (i.e., 45, 135, 225 and 315 degrees), the image comparisons are poor; only a general match on the overall silhouette of the target is obtained between the measured and computed images. Note that the silhouettes of the measured images are well-defined and are quite similar to those obtained in the computed images; this suggests that any ground-target interaction effects in the real measurement are minimal, and the omission of ground-target interaction in the computation is justified.

The generally poor agreement between the measured and computed images of the BTR70 is quantitatively summarized by the cross-correlation scores in Table 1. The cross-correlation scores are very low at all viewing angles. The scores provide a measure of the degree of similarity based on the amount of pixel intensity overlap between the measured and computed images. As an example, a measured image cross-correlates against itself will produce a maximum cross-correlation score of 1.0, implying a very high degree of similarity between the two images.

*Table 1: Cross-correlation scores as a function of azimuth angle for the BTR70.*

Azimuth angle (degrees)	Cross-correlation score
1	0.37
43	0.24
91	0.29
131	0.22
179	0.36
227	0.29
274	0.31
317	0.23

Besides using the whole target image as the feature for analysis, strong scatterers that appear in the measured images can potentially be used as characteristic features to identify a target; however, some of these scatterers can vary considerably in pixel intensity, and can even disappear by changing the viewing angle by only a very small amount. This can cause difficulties in obtaining consistent comparisons between measured and computed images, especially when ground truth information of the measured images is not available. An example is illustrated in Figure 7 (left hand column). A sequence of measured images is shown in which the BTR70 has rotated just a couple of degrees in either direction in the azimuth about the head-on aspect position. It is seen that two strong scatterers at the back of the vehicle (indicated by the arrows in the middle image) fade away quickly as the viewing angle is rotated slightly; these scatterers correspond to the hatch door areas of the engine compartment at the rear of the vehicle. The cause of the fading is not clear; it is likely the results of the complex geometry of the actual target at these particular locations. In the computed images shown in Figure 7 (right hand column), the two scatterers that represent the hatch door areas persist in the images through the viewing aspect rotation. This can be explained by the fact that these two scatterers in the computed images are modelled as trihedral corners in the CAD model; the trihedral representation of the hatch door area is seen in Figure 8. A trihedral tends to have a retro-reflecting property; that is, it will reflect radiation back along the original direction. In this particular case, the trihedral corners may be an over-simplification in the representation of the hatch doors. This fading behaviour of prominent scatterers over a small change in viewing angles is observed regularly in SAR images of real targets. More examples of this fading behaviour in the SAR images of another vehicle will be discussed in the next section.

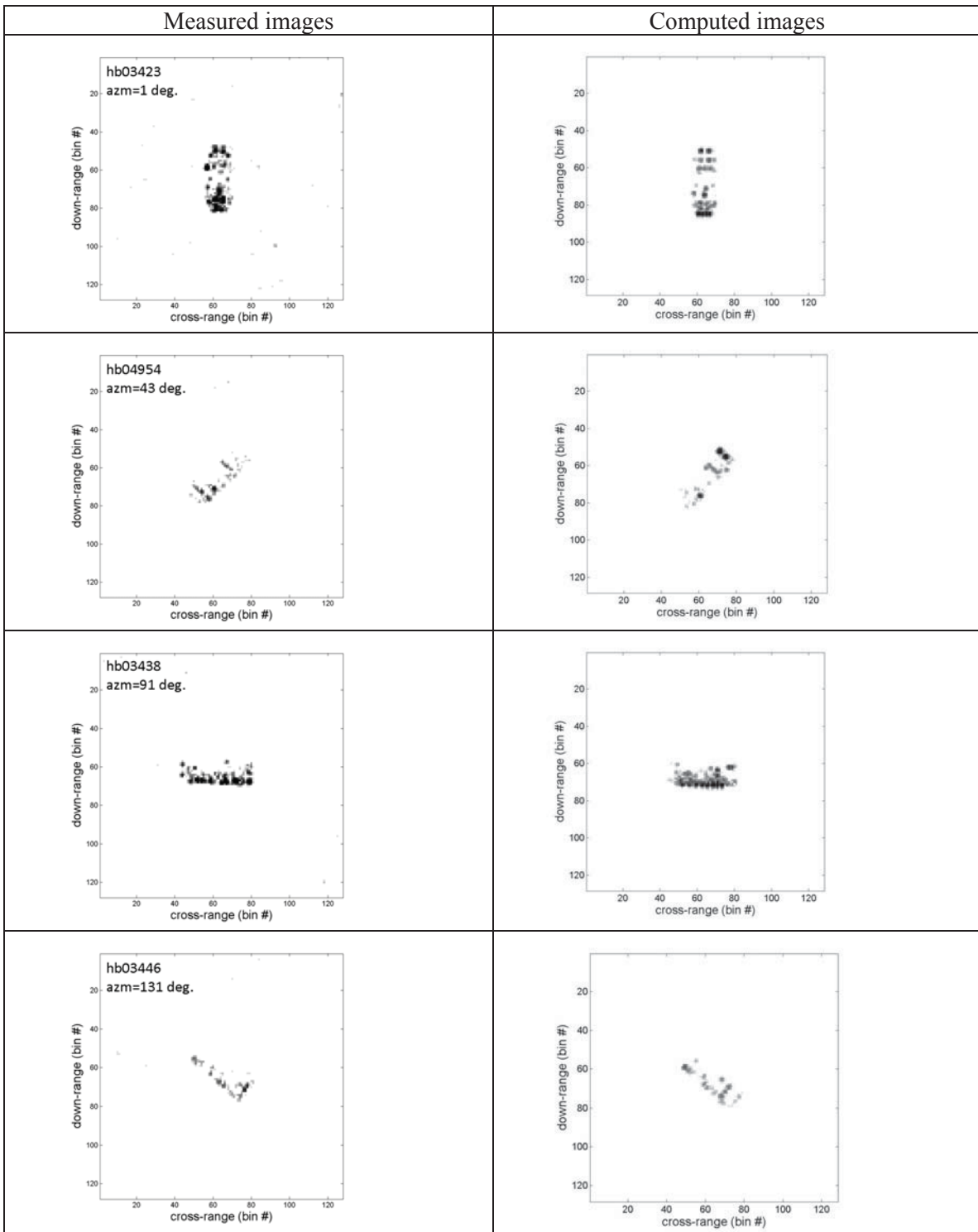


Figure 6: comparisons between measured and computed SAR images of the BTR70.

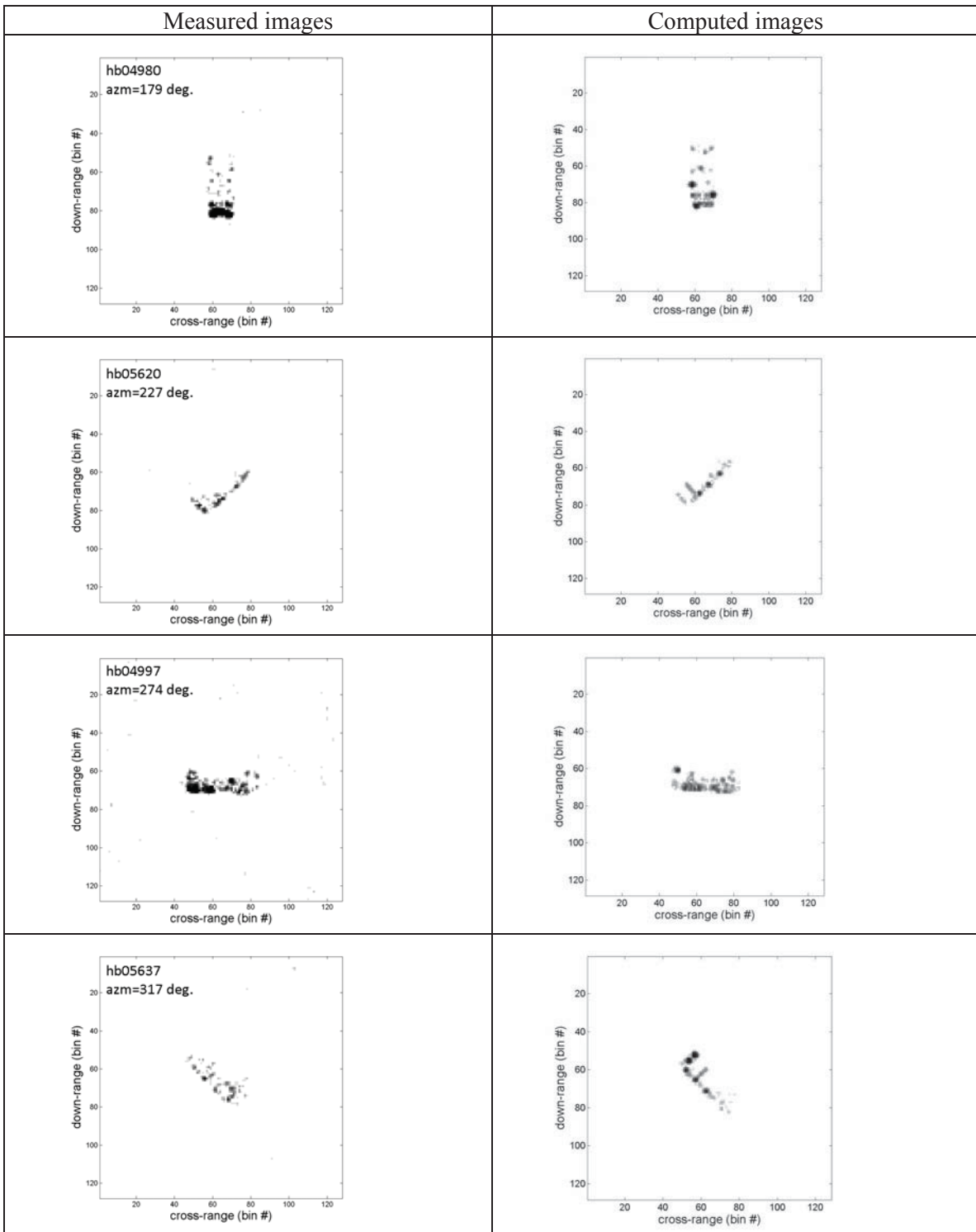


Figure 6: continued.

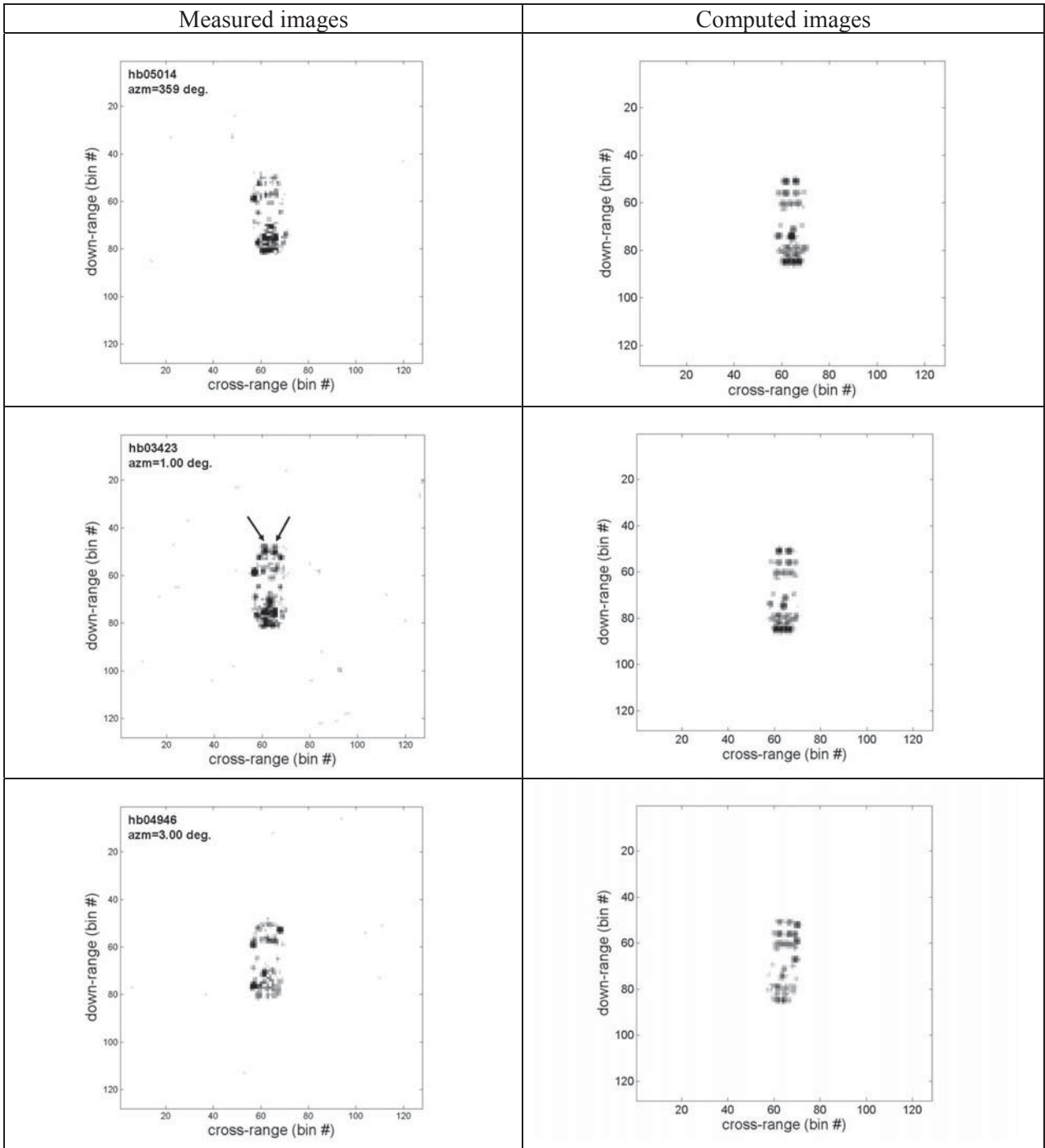


Figure 7: Comparisons between measured and computed SAR images near head-on aspect viewing angles.

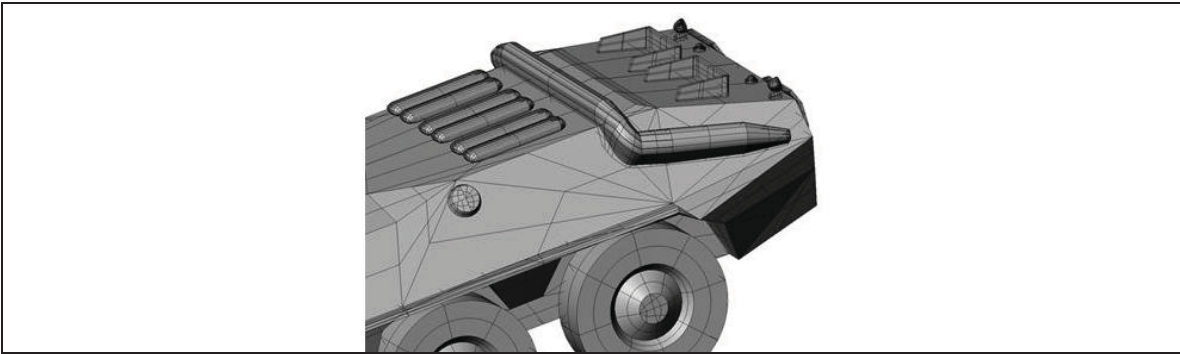


Figure 8: CAD model of engine compartment hatch doors.

## 4.2 Gvozdika, self-propelled howitzer

In computing the Gvozdika, the tracks for the track-and-wheel drive of the vehicle are not modelled in the CAD model. A picture of the track-and-wheel drive on a Gvozdika is shown in Figure 9. Because of the complex mechanical design of the tracks, it is anticipated that the scattering from the tracks will be a diffused process, and the backscattering would not have any significant contribution to the image. Furthermore, the geometrical complexity of the tracks could introduce undesirable artefacts in the computation; this is based on experience in dealing with computing scattering from a large number of very small pieces clustered together on a target. The comparisons between the measured and the computed SAR images of the Gvozdika self-propelled howitzer over 360 degrees in azimuth are shown in Figure 10. The comparisons are in fair agreement visually for the silhouettes of the target at most viewing angles. A more quantitative evaluation of the comparisons is given by the cross-correlation scores in Table 2. The scores indicate that better agreement is obtained with the Gvozdika images than those of the BTR70. A contributing factor to the better comparative results can be attributed to the simple shape of the Gvozdika. The geometrical profile of the target is relatively simple and clean (i.e., no complicated contours) as seen in the photo in Figure 3.



[www.militaryfactory.com/imageviewer/ar/picdetail.asp?armour\\_id=88&sCurrentPic=2s1gvozdika\\_4.jpg](http://www.militaryfactory.com/imageviewer/ar/picdetail.asp?armour_id=88&sCurrentPic=2s1gvozdika_4.jpg)

Figure 9: Gvozdika's track-and-wheel drive.

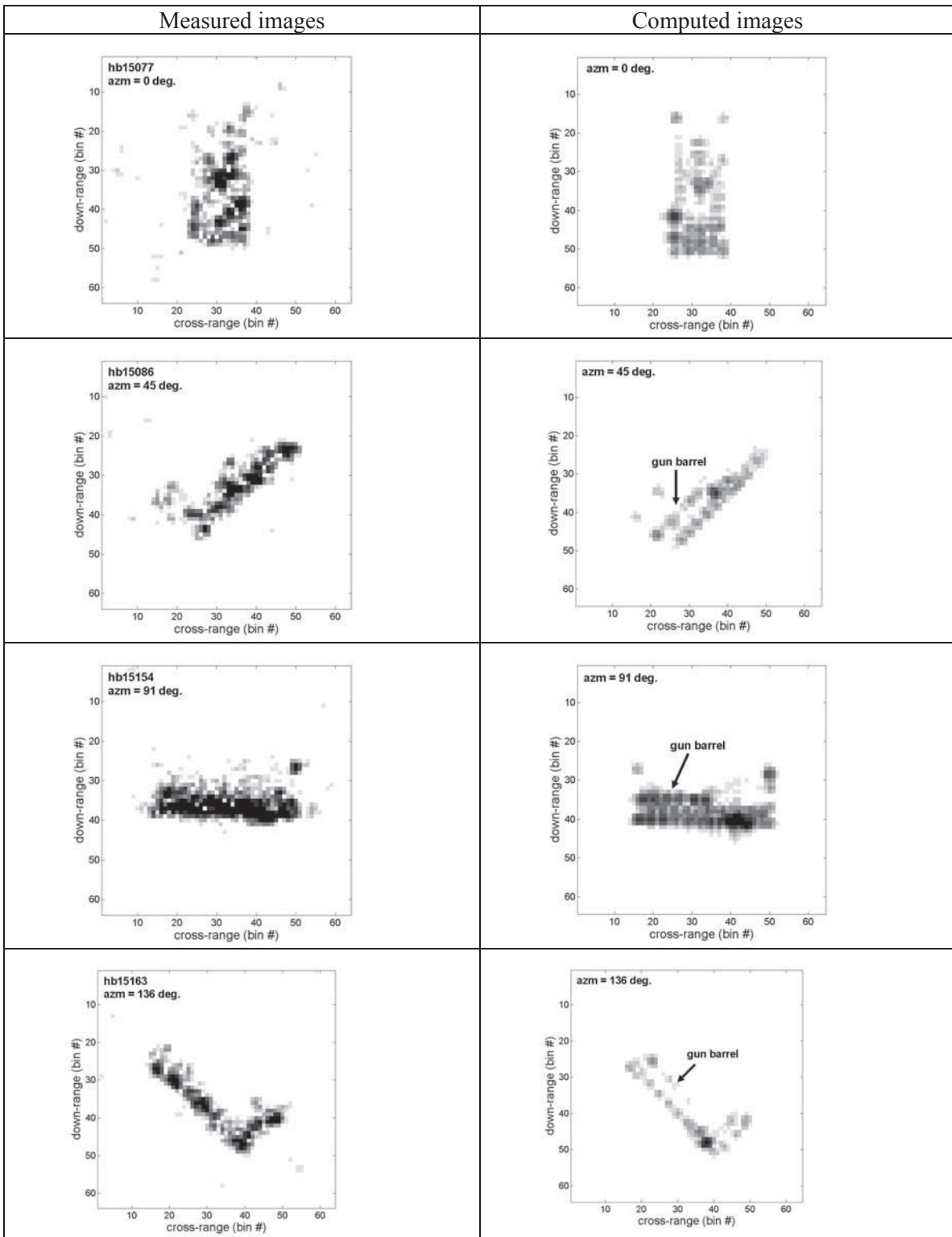


Figure 10: Comparison between measured and computed SAR images of the Gvozdika.

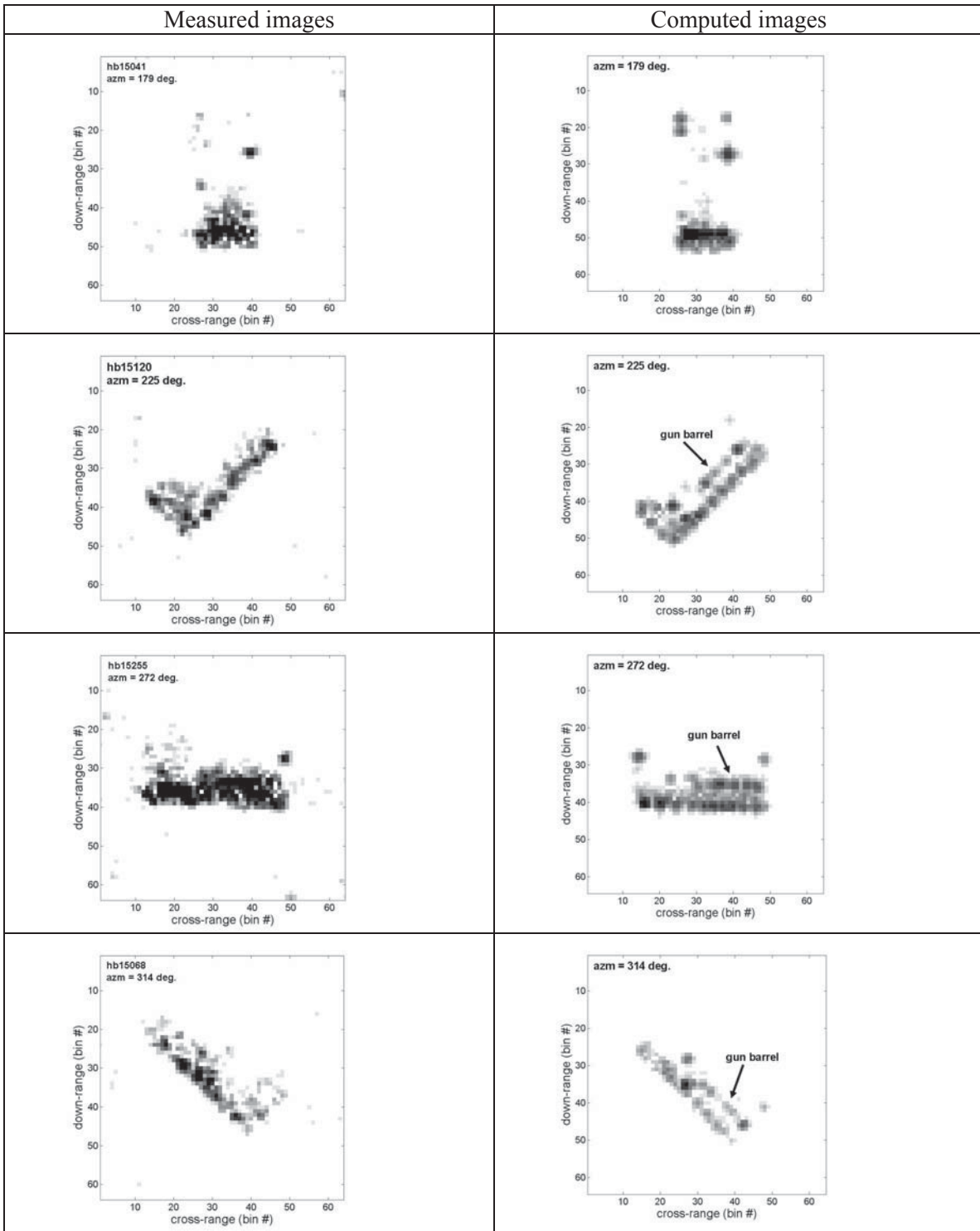


Figure 10: continued.

Table 2: Cross-correlation scores as a function of azimuth angles for the Gvozdika.

Azimuth angle (degrees)	Cross-correlation score
0	0.43
45	0.39
91	0.49
136	0.43
179	0.31
225	0.35
272	0.47
314	0.35

As in the case of the BTR70, there are some scatterers that fade in and out quickly with a slight rotation of the viewing angle in the measured SAR images of the Gvozdika. This is illustrated in Figure 11 at head-on aspect viewing angle. In the measured images on the left-hand column of Figure 11, the scatterer on the left side of the target (highlighted by the dashed circle) fades out completely as the viewing angle is rotated from -2 degrees to 2 degrees in the azimuth. This scatterer represents the engine exhaust manifold piece as shown in the photo in Figure 12. In the CAD model, the exhaust manifold is represented by a simple structure, as shown in the bottom figure of Figure 12. The box structure creates a dihedral-like scatterer at this target location. The computed images of the Gvozdika are illustrated on the right-hand column of Figure 11. In the computed images, there is a reversal in the fading behaviour of the scatterers that represent the exhaust manifolds. The manifold scatterer on the right-hand side is gaining intensity as the viewing angle is rotating from -2 to 2 degrees in the azimuth. The two exhaust manifolds are symmetrically located on the CAD model. The cause of the discrepancy in the scattering behaviour between the measured and computed images is not clear.

Similar behaviour is observed at other locations on the Gvozdika where scatterers are seen fading out quickly by rotating the viewing angle a few degrees in the measured image. This is shown in Figure 13 (left column) where the two scatterers representing the back sides of the headlight covers at the front of the vehicle fade out almost completely as the azimuth viewing angle is changed from 182 degrees to 178 degrees (i.e., tail-on aspect). The faded scatterers are highlighted in the dashed rectangular window. A picture of the headlight assembly on a Gvozdika is shown in Figure 14 (top). In the computed images, the scatterers correspond to the back-side of the headlight persist over the same azimuth angles without fading away. This is shown in Figure 13 (right column). The back-side of the headlight assembly is modelled as part of a dihedral with the target's body; the CAD model of the headlight assembly is shown in the bottom figure of Figure 14 (bottom). The fading behaviour of some of the strong scatterers by changing the viewing angle by only a small amount introduces difficulties in establishing them as well-defined target features for a reference database; what this means is that these prominent scatterers at specific locations, which are useful as reference markers for a particular target type can not be relied upon. To make matter worse, the computed fading behaviours of these scatterers are opposite to what are being observed in the measured data. This renders the headlight scatterers not useful as target features to be stored in a reference database.

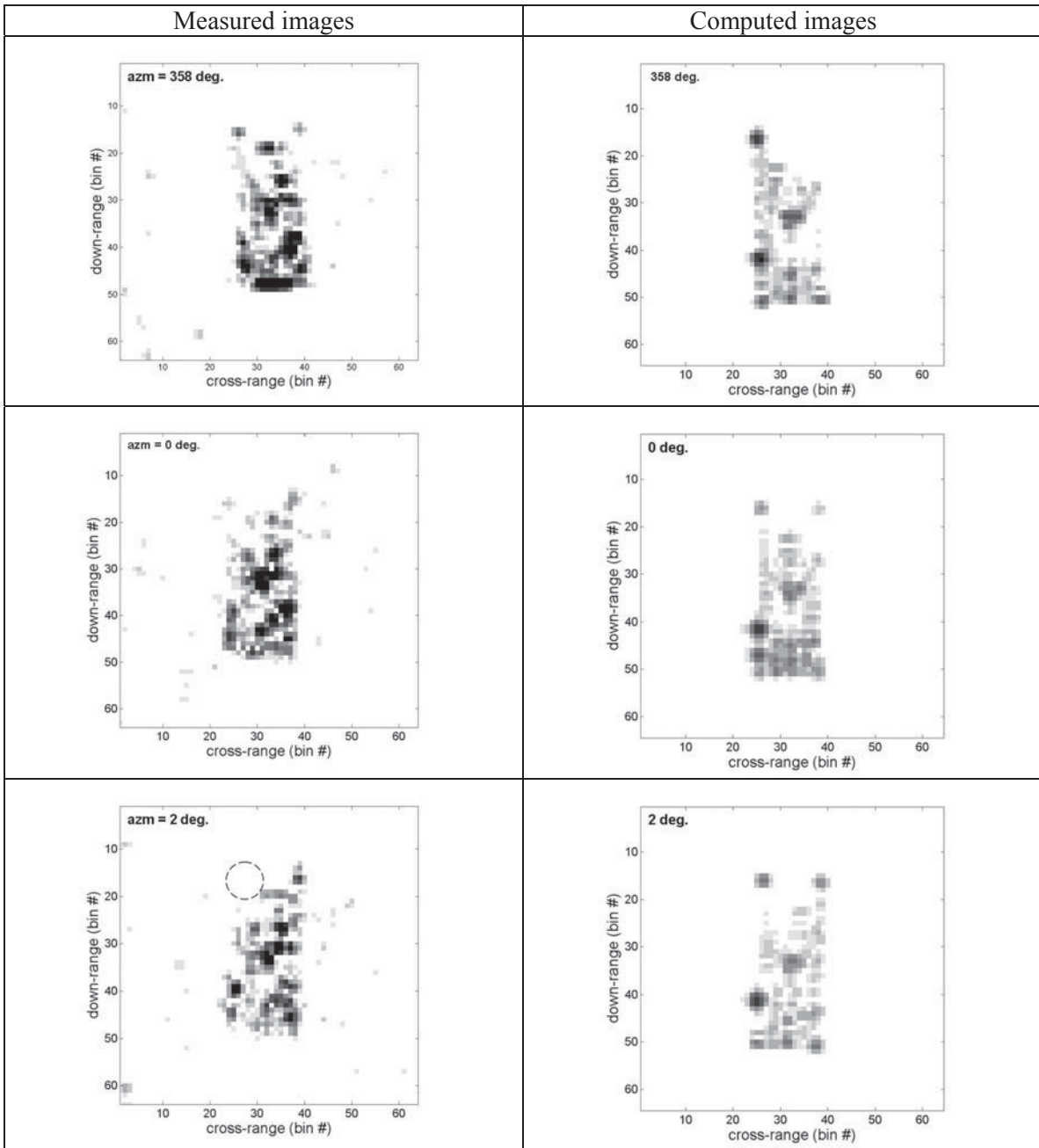


Figure 11: Comparisons between measured and computed images at head-on aspects.

A distinct feature on the Gvozdika is the long gun barrel. However, the gun barrel does not show up very well in the measured images as seen in Figure 10. But the scattering from the gun barrel is visible in the computed images; the gun's image is indicated in Figure 10 (right column). Using the computed images as reference, one can infer the presence of the gun barrel in the measured images in Figure 10 (left column), although the correspondence is not strong or obvious by visual inspection. With some training, human analysts could be trained to recognize distinct features to make a high-probability verification of a specific target. Even if the computed images are not of

high fidelity, they may still be useful as reference guides when seeking a specific target. The human's innate cognitive ability can be cued to extract any distinct feature from the measured images that offer relevant information about a specific target of interest. As example, the gun barrel can be readily interpreted in the measured images at 91, 136, 272 and 314 degrees on the left column of Figure 10 after comparing with the computed images on the right column at the same azimuth angle.

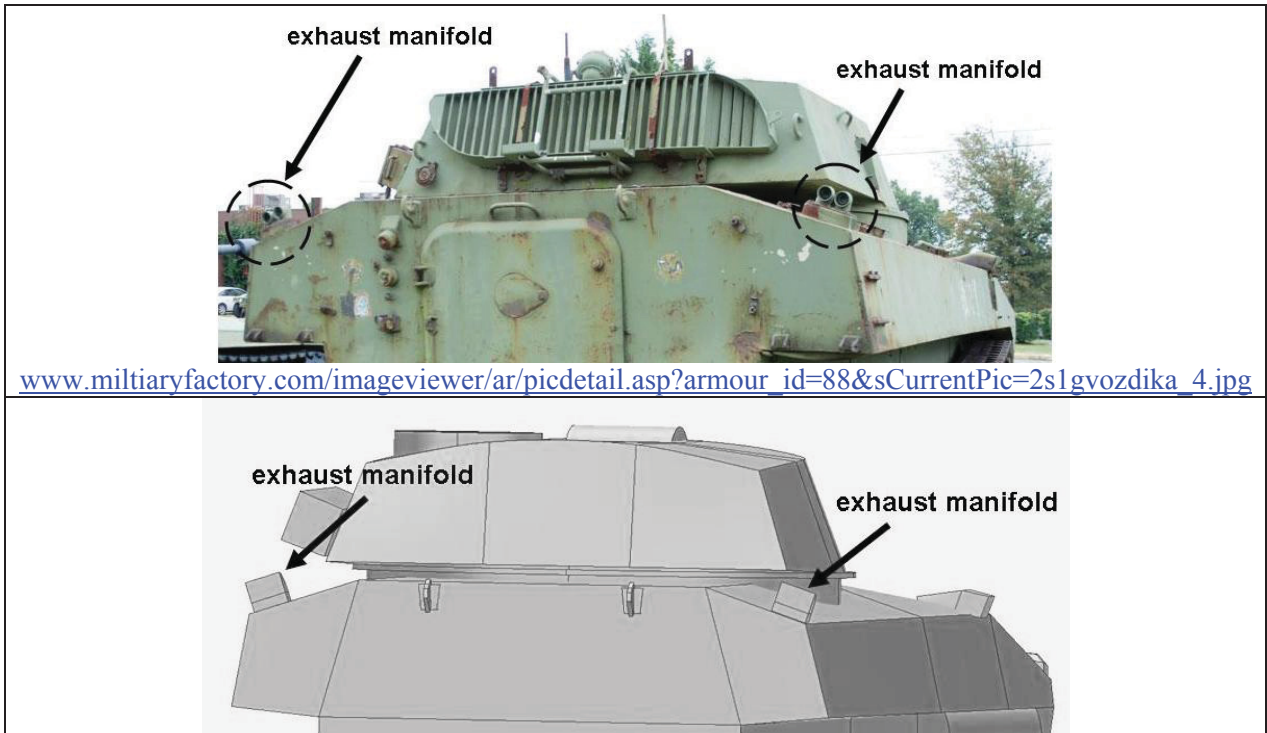


Figure 12: Photo of the exhaust manifolds on a Gvozdika (top), CAD model of the exhaust manifolds (bottom).

Overall, there is a fair general agreement on the silhouettes between the computed and measured images, even though the computed images do not compare very well against the measured images on a pixel-to-pixel basis. The general similarity in the silhouettes can be exploited by human analysts in a target verification process; the silhouettes would be distinct for specific target types [10].

The lack of precise agreement between the measured and computed images could be an indication of the inadequate quality of the CAD model of the target. From a previous study using a simple canonical target (SLICY), excellent agreements were obtained in the comparison between the measured and computed SAR images over 360 degrees in azimuth [9]. This is illustrated in Figure 15. Because of its simple geometry, the CAD model is able to represent the SLICY target quite accurately, allowing high fidelity SAR images to be computed. In the case of the Gvozdika, the target's shape is more complex. The CAD model of the Gvozdika may not have provided a highly accurate representation of the target's actual shape to support computation of good quality images.

The issue of CAD model accuracy in representing the scattering characteristics of a target is an area that is not very well documented in the open literature; this is partly due to the potential for military application of the subject. Often, the targets of interests under study and evaluation are operational targets; this severely limits the accessibility of the information due to classification restrictions. An examination on the issue of CAD model accuracy is further discussed in the next section.

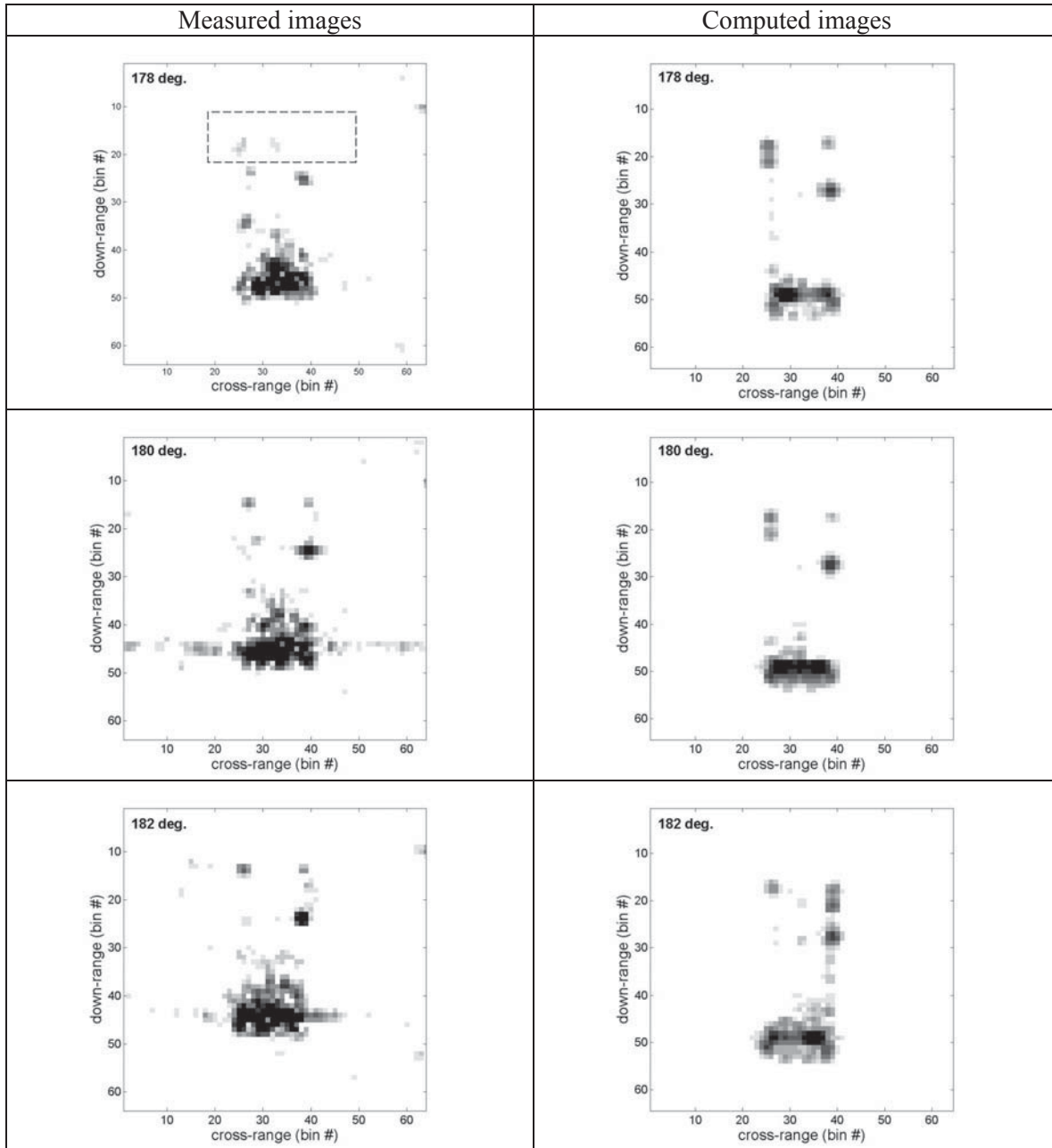
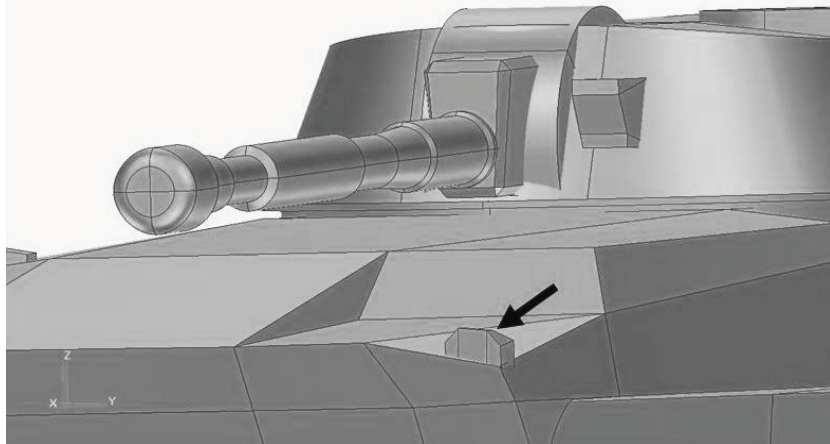


Figure 13: Comparisons between measured and computed images of the Gvozdika at tail-on aspect.



[http://asian-defence-tech.blogspot.com/2011/03/2S1-gvozdika-wallpapers\\_9275.html](http://asian-defence-tech.blogspot.com/2011/03/2S1-gvozdika-wallpapers_9275.html)



*Figure 14: Photo of the headlight cover on the Gvozdika (top), CAD model (bottom).*

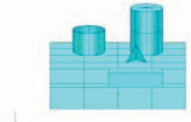
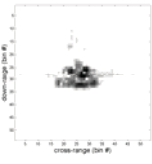
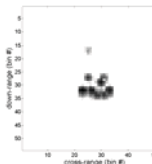
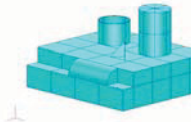
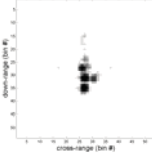
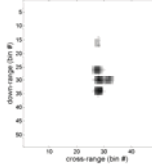
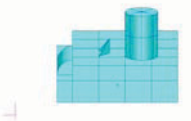
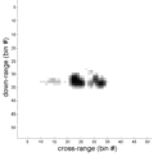
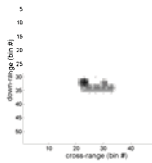
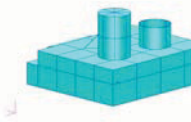
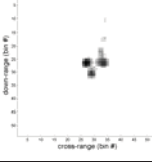
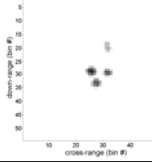
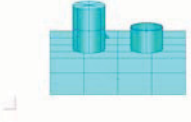
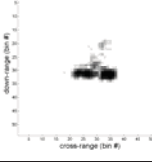
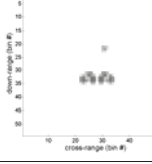
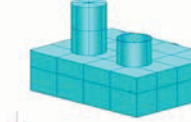
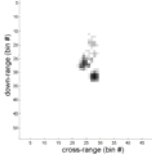
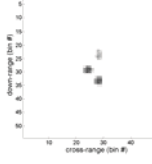
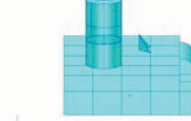
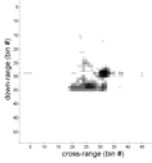
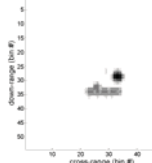
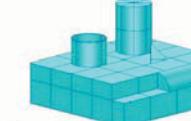
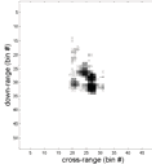
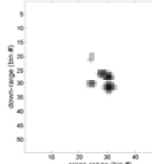
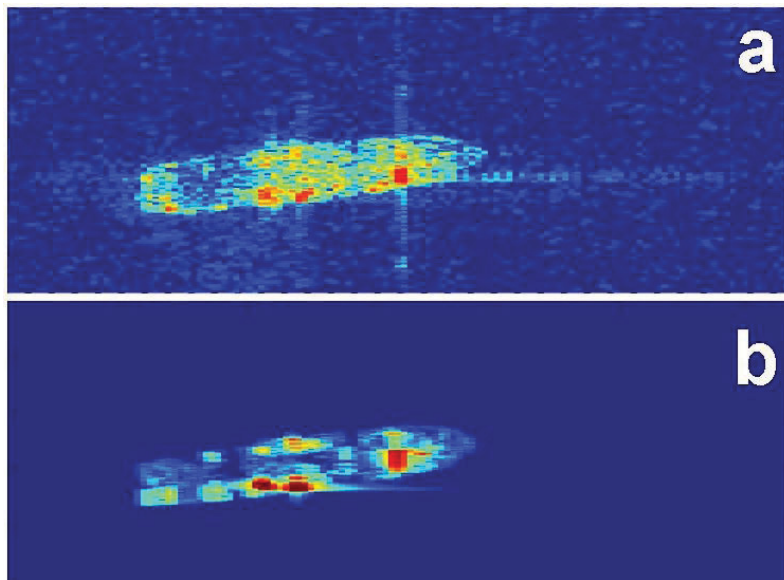
Azimuth viewing angles	Measured data (file #)	Computed images
 0 deg	 hb15238	
 45deg	 hb15049	
 90deg	 hb15254	
 135deg	 hb15197	
 180deg	 hb15076	
 225deg	 hb15144	
 270deg	 hb15152	
 315deg	 hb15032	

Figure 15: Comparisons between measured and computed images of a canonical target [11].

### 4.3 Naval warships

SAR images of two naval warships of the same vessel type are available in the RADARSAT2 SAR imagery archive. The images were captured in spotlight mode from anchored stationary vessels at an incidence angle of 30.5 degrees and at a couple of different viewing azimuth angles. Figure 16a shows the measured SAR image of one of the warships at an azimuth angle of 5.9 degrees to the starboard side. The warship vessel-type will not be revealed in order to comply with the classification designation of this document. Two CAD models of the warship are available for SAR image computation. One of the CAD models was built from engineering drawings of the warship, and is therefore considered as containing high precision geometrical details of the target. The second model came from a commercial source. The accuracy of the target's geometry of this CAD model is not known. Most commercial CAD models are visual look-alike model that are used mainly for computer graphic animation, and are not intended for scientific computing purposes. Thus, the commercial CAD model is not expected to be of high precision in the technical details.

The comparison between the measured and computed SAR images using the high-precision CAD model is shown in Figure 16. It is seen that the computed image displays all the major scattering sites of the warship that are also seen in the measured image; however, the finer details are not comparing well between the two images. To give a more quantitative measure of the comparison, a cross-correlation is performed between the measured and computed images in Figure 16; a score of 0.79 is obtained. The scores indicates that there is a relatively good match between the two images.



*Figure 16: Comparison between measured image (a) and computed image (b) of a naval vessel using a high-precision CAD model. Incidence angle = 30.5 deg., azimuth = -5.9 deg.*

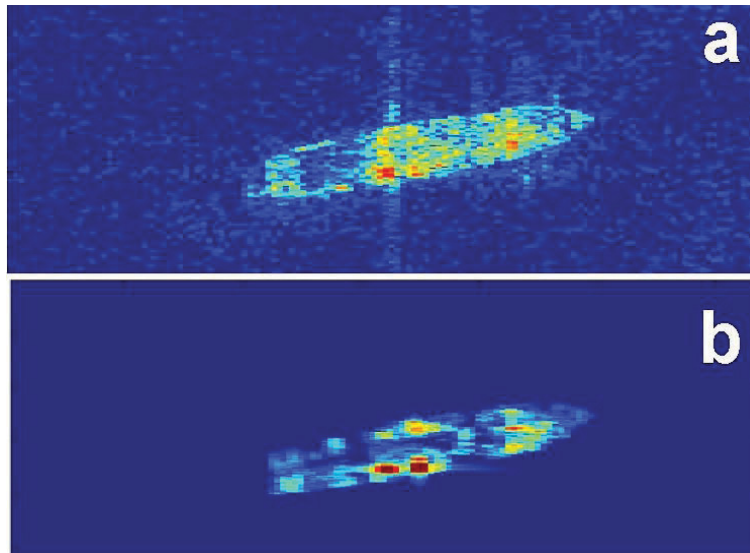


Figure 17: Comparison between measured image (a) and computed image (b) of a naval vessel using a high-precision CAD model. Incidence angle = 30.5 deg., azimuth = -8.4 deg.

The measured SAR image from a second warship of the same vessel class viewed at an azimuth angle of 8.4 degrees to starboard is compared with computation; the comparison is shown in Figure 17. The agreement is also good, with all the major scattering sites predicted by the computed image; a cross-correlation score of 0.73 is obtained between the measured and computed images.

The poor agreement in the fine details in the comparisons of both Figure 16 and Figure 17 can be attributed to the lack of deck clutter modelling in the CAD model of the warship. Real naval vessels usually have a large amount of deck clutter that is different from ship to ship. The deck clutter includes wrenches, cable spools, air scoops, life rafts, small weapon mounts and equipment accessories. It is difficult to include all the deck clutter into the CAD model in a meaningful manner unless detailed information of the deck clutter of a specific ship is given. Otherwise, the CAD model can only provide an overall description of the ship's general geometry. Moreover, the clutter details may only contribute relatively weak scattering compared to the major scattering sites from the ship's superstructure. Smaller bright pixels reminiscent of clutter scattering can be seen in the measured images in Figure 16 and Figure 17. In the computed images, the CAD model does not include any deck clutter modelling; hence returns from backscattering off smooth flat surfaces tend to be low level, and uniformly flat in pixel intensities.

How the accuracy of the CAD model may affect the fidelity of the computed target image has always been an issue. To address this issue, a second CAD model of the warship from a commercial source is used for SAR image computation. The commercial CAD model is not expected to be of high precision in the physical details. A comparison between the measured and computed images of the warship at a viewing azimuth angle of 5.9 degrees to starboard is shown in Figure 18. It is seen that most of the major scattering sites present in the measured image are also predicted by the computed image; however, the computed image has failed to predict one major scattering site at the front section of the ship. The missing prominent scatterer in the computed image is clearly evident in Figure 18b.

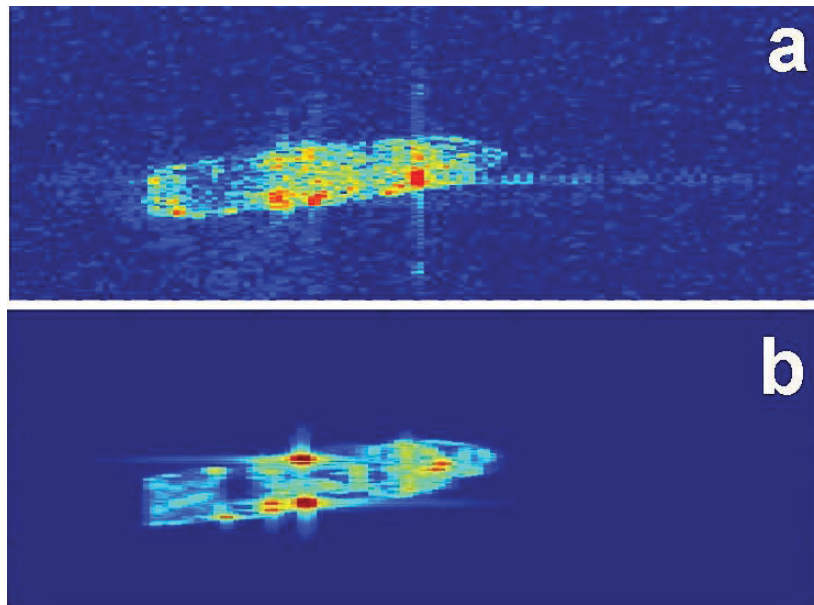
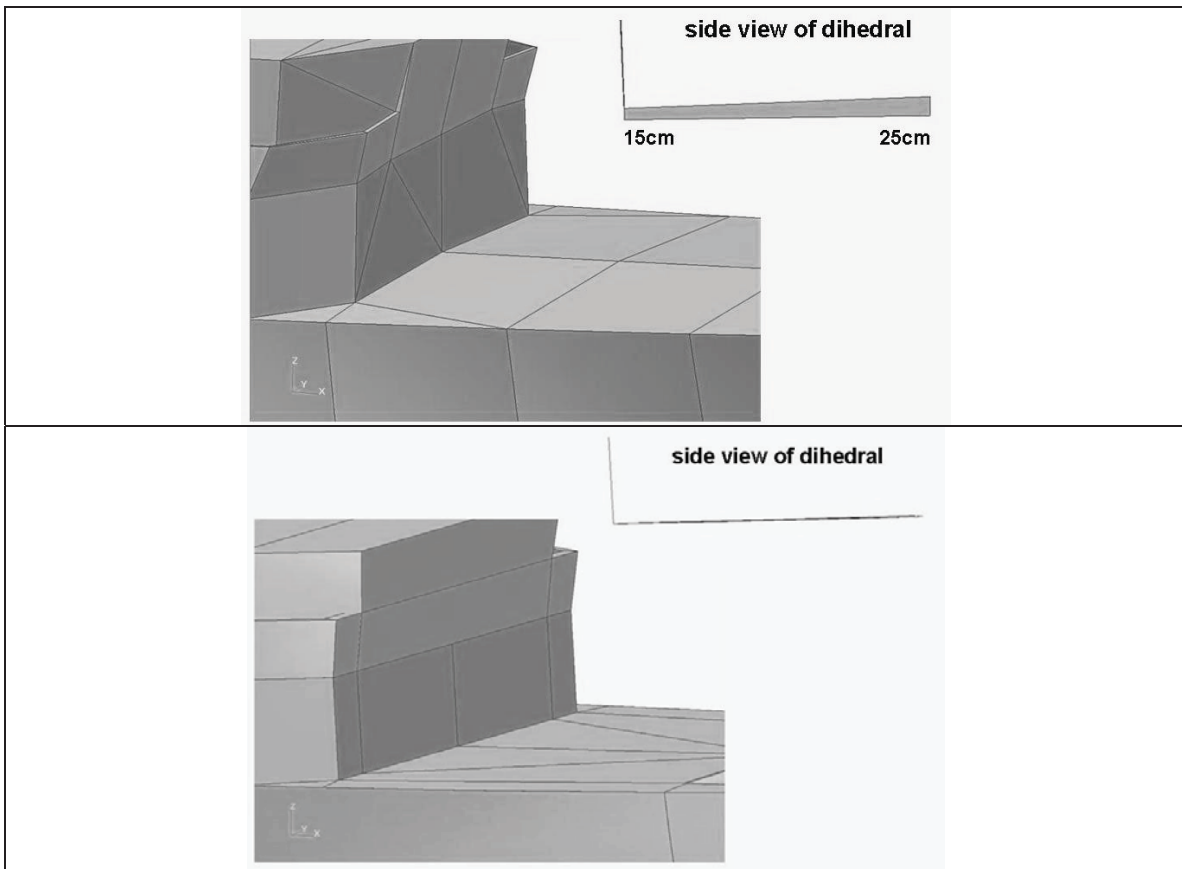


Figure 18: Comparison between measured image (a) and computed image (b) using a commercial CAD model. Incidence angle = 30.5 deg., azimuth angle = -5.9 deg.

The location of the missing scatterer is traced to a dihedral corner formed between the wall of the superstructure and the deck floor just below the bridge of the ship. Illustrations of the dihedral location from both the precision CAD model and the commercial CAD model of the warship are shown in Figure 19. There is clearly a difference in the dihedral structures between the two CAD models. It can be seen that the deck floor in the precision CAD model is buckled upward slightly by a very small amount; in the commercial CAD model, the deck floor is modelled as a flat surface. Thus, the scattering behaviours between these two slightly different dihedral structures would be expected to be different in the computation.

To examine the scattering characteristics of these two slightly different dihedral structures, the dihedral site is extracted from each of the two CAD models. They are then computed in exactly the same manner at a number of azimuth viewing angles near the head-on aspect. The results of the computed SAR images from both dihedral structures are shown in Figure 20. It is clearly seen that as the azimuth viewing angle is rotated a few degrees to the starboard side, the SAR images of the two dihedrals are markedly different. As the azimuth viewing angle is increased beyond 3 degrees towards the starboard side, the scattering intensity of the dihedral from the commercial CAD model is fading rapidly; whereas, the scattering of the dihedral from the precision model remains quite strong. Moreover, in the high-precision CAD model, the scattering image appears only from the starboard half of the dihedral structure; this is shown in the third image on the left hand column of Figure 20. This computed image of the dihedral structure is the same as that of the measured image of the warship in Figure 16. In the measured image of the ship, the dihedral located just below the bridge of the ship is also seen to exhibit scattering from the starboard half only. This observed scattering behaviour can be explained by the slightly convex shape of the deck floor. Because of the curvature of the deck floor, scattering from the port side half of the dihedral structure is deflect to the port side direction. Hence, scattering from the port side half of the dihedral does not contribute to the image at the bridge location when viewed at a starboard

aspect angle. The convex shape of the ship's deck floor deviates only by a very small amount from a flat surface, buckling upward by just 15 to 25 cm across a width of about 16m; this is illustrated in the broadside view of the dihedral structure in Figure 19. This deviation is less than 1.5% from a perfectly flat surface. This small amount of deviation in the deck's surface is apparently sufficient to influence the scattering process and has a significant impact on the appearance of the ship's SAR image. In contrast, the scattering from a dihedral made up of two flat surfaces fades away with increasing azimuth angle. This is seen from the image in the third row of Figure 20. Thus comparisons of the computed SAR image from the two slightly different dihedral structures has clearly demonstrated that the accuracy in the physical details of a CAD model can have a big effect in the fidelity of the computed images. In this case, it is shown that an adverse effect can come from even a small structural deviation of a very simple geometrical structure.



*Figure 19: Dihedral structure formed at the bridge location of the vessel; top: high-precision CAD model, bottom: commercial CAD model.*

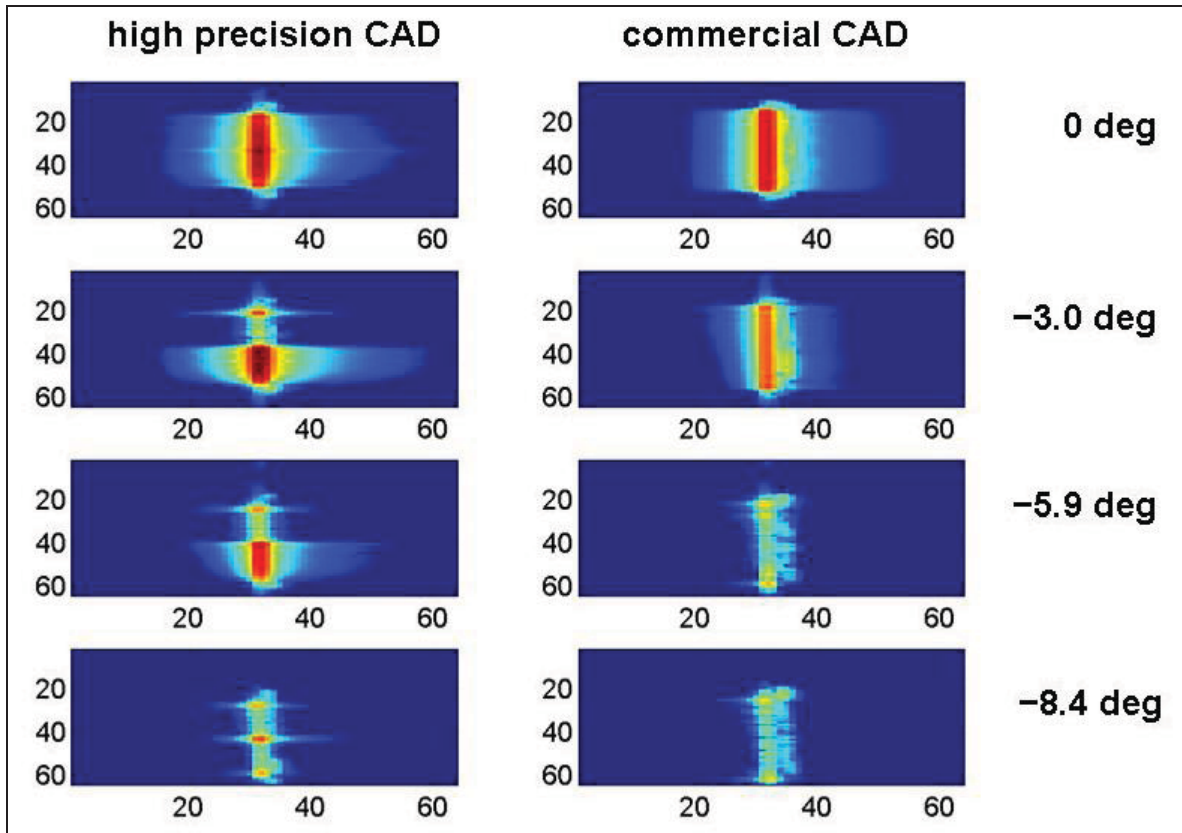


Figure 20: Comparisons of the bridge dihedral structure scattering behaviour between the high-precision CAD model and the commercial CAD model at different azimuth angles; the negative sign indicates viewing from the starboard side. Horizontal:down-range; Vertical:cross-range

#### 4.4 “Alboran”, a catamaran ferry

Two RARADSAT2 images of the catamaran ferry “Alboran” are used for comparing against the computed images. Figure 21 shows the two measured SAR images of the Alboran; the ferry was docked at a terminal. Thus there is some land clutter present in the measured SAR images.

The ferry in Figure 21a was imaged at an incidence angle of 48.4 degrees. Since there is no information on the orientation of the ferry in the measured data, the image of the ferry could have two possible interpretations of the viewing angles, 28 degrees to the starboard side viewing from the front of the ferry, or 152 degrees to the port side viewing from the rear of the ferry. These two ferry orientations are illustrated in Figure 22. The corresponding comparisons between the measured and computed images are shown in Figure 23 and Figure 24. In Figure 23, the computed image is viewed from the front of the ferry, and in Figure 24, the computed image is viewed from the back of the ferry. It is seen that there is little resemblance between the computed images and the measured image from neither viewing angles.

In the second measured SAR image (Figure 21b), the ferry was imaged at an incidence angle of 34 degrees. The azimuth viewing angle is about 45 degrees to the starboard side. The front of the

ferry is determined to be pointing upward in Figure 21b. This is deduced from the location of the two rotating antennas that can be seen in the measured image. The computed image is shown in Figure 25b. It is seen that there is again poor agreement between the measured and computed SAR images. The measured image (Figure 25a) seems to have the front section of the ferry missing; there is little or no scattering return from the bow section. Both the measured and computed images in Figure 25 have the same physical scaling (1-to-1) in both range (horizontal) and cross-range (vertical) directions. Thus both images are of the same size. Based on the identical window size of the two images, the absence of the bow section in the measured image is evident.

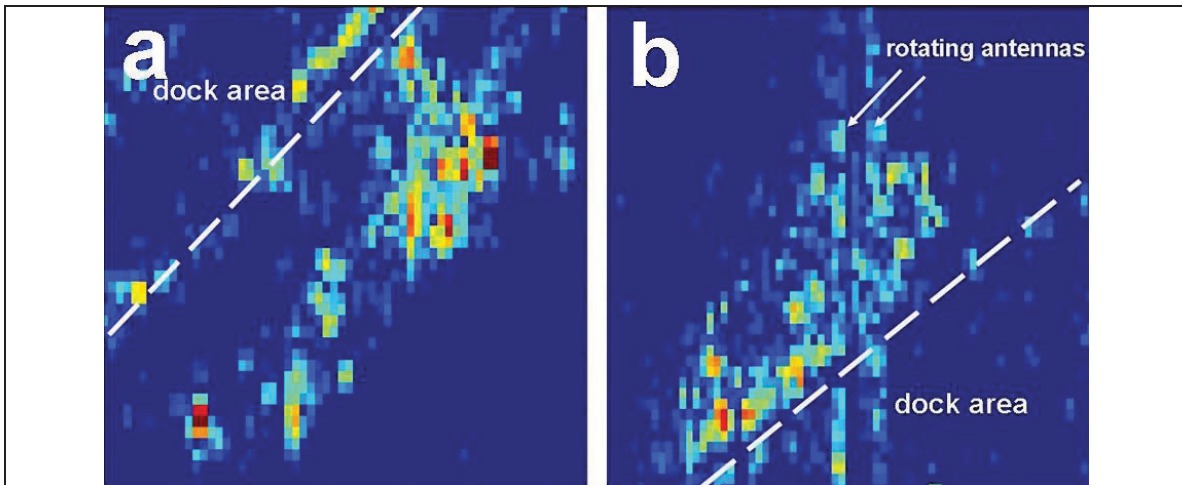


Figure 21: Two measured SAR images of the catamaran ferry, “Alboran”; image captured at: a) incidence angle = 48.4 deg, b) incidence angle = 34 deg.

One explanation that could be used to account for the discrepancy is the quality of the CAD model used in the computation. The CAD model of the ferry is a commercial model of unknown accuracy in the physical details. A visual inspection and comparison of the photo of the Alboran in Figure 4, and the CAD model of the ferry in Figure 5 indicate that the CAD model may not be providing an accurate portrait geometrically of the Alboran. From the photo of the Alboran, the actual profile of the ferry appears to be sleeker than that of the CAD model, especially the bow section; the CAD model looks stubby in comparison. The distance from the tip of the bow to the front of the passenger cabin, and the location of the pilot’s bridge to the front of the cabin also look out of portion between the photo and the CAD model. The poor match between the measured and computed images of the bow section as shown in Figure 25 suggests that the CAD model may not be modelling the bow section of the ferry properly. The poor agreement of the comparisons with two different measured images indicates that the CAD model of the ferry might be a source of the problem.

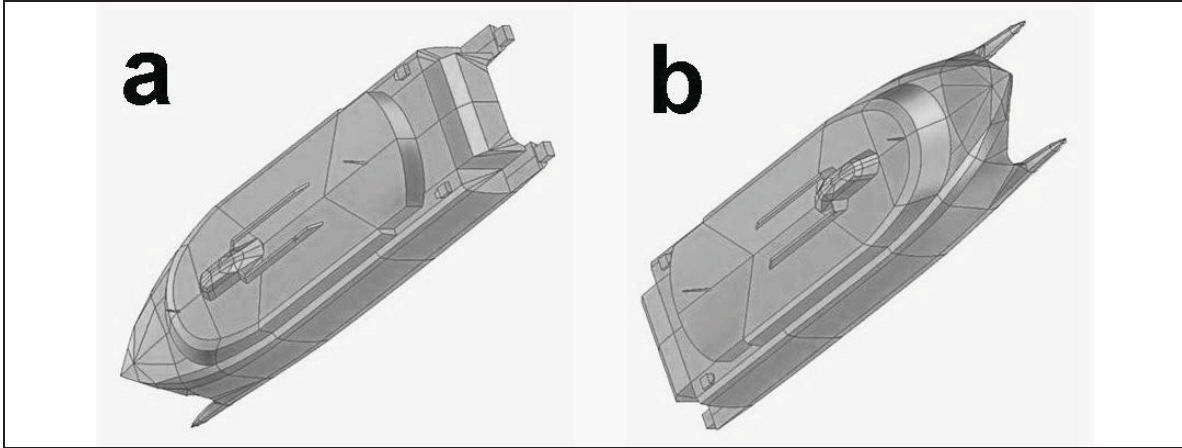


Figure 22: Optical views of 2 possible orientations of the SAR images of the docked ferry in Figure 21a; a) azimuth = 152 deg., b) azimuth = -28 deg.

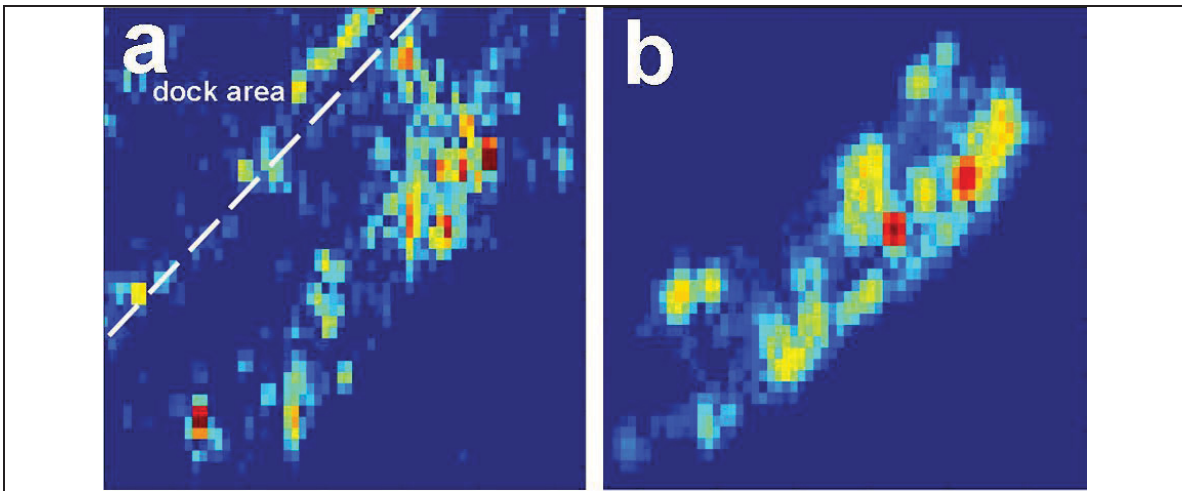


Figure 23: Comparison between the measured image (a) and the computed image (b) of the ferry. Computed image: incidence angle = 48.4 deg., azimuth angle = -28 deg (viewed from the front of the ferry).

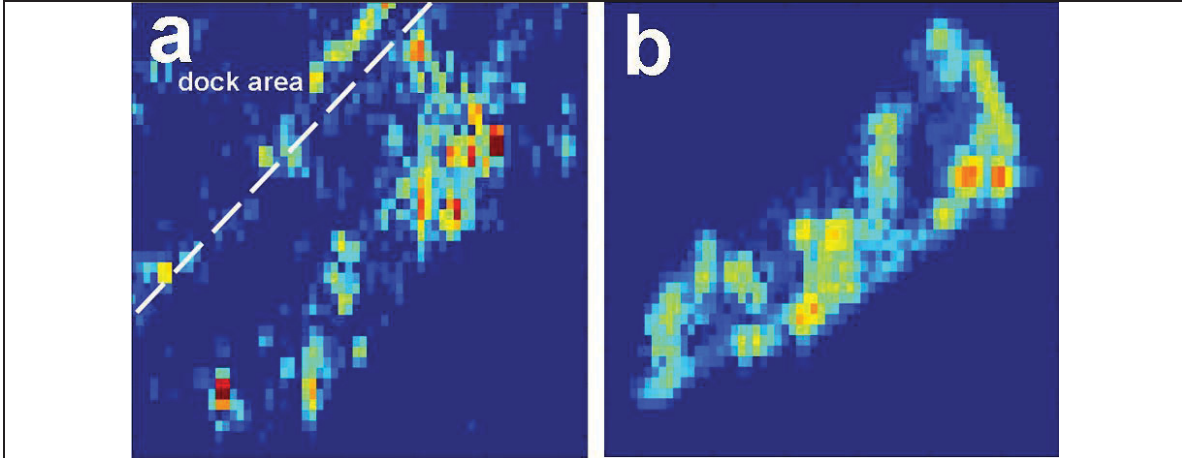


Figure 24: Comparison between the measured image (a) and the computed image (b) of the ferry. Computed image: incidence angle = 48.4 deg., azimuth angle = 152 deg (viewed from the back of the ferry).

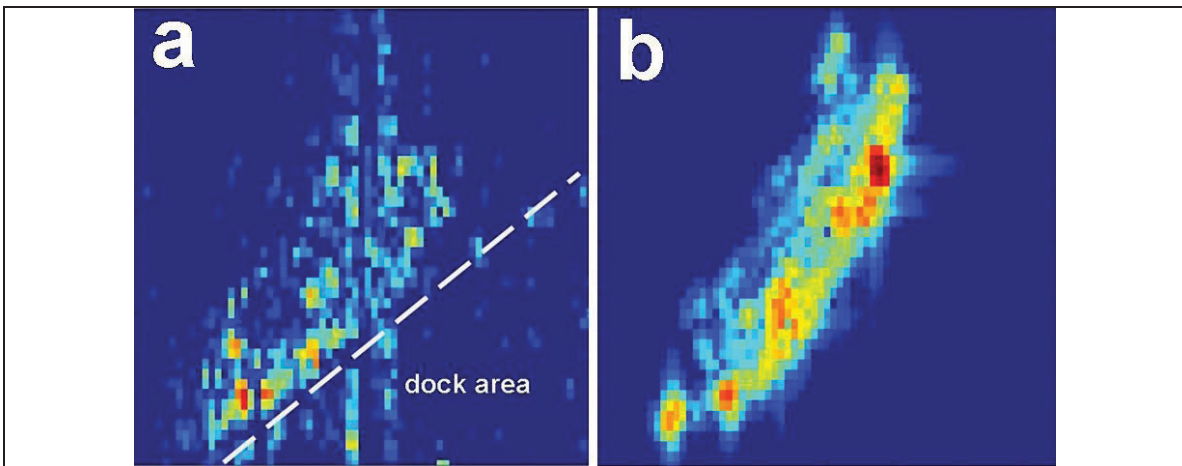


Figure 25: Comparison between the measured image (a) and the computed image (b) of the ferry.

## 5 Conclusions

---

Investigation on the quality of the computed SAR images is carried out using four real complex targets: two land vehicles and two naval vessels. Comparisons between measured and computed images are conducted to determine the fidelity of the computed images. A cross-correlation method is also used to provide a quantitative measure of image fidelity. For the two land vehicles, results indicate that the fidelity of the computed images is rather poor on a pixel-to-pixel basis. But the general overall patterns of the image silhouettes are in reasonably good agreement between the measured and computed images. This suggests that the target silhouettes could serve as useful target features.

For the warship, good agreement is obtained for a group of major scatterers on the target between the measured and computed images. The spatial distribution patterns of these scatterers can be used as unique signatures for the warship. By using two CAD models of varying accuracy to assess the computed images of the warship, results from the comparative analysis indicate that the accuracy of the CAD model has a considerable impact on the fidelity of the computed images. The problem of CAD model accuracy in generating acceptable quality computed images is also encountered when analyzing the catamaran ferry.

The comparative analysis conducted in this study also offers some insights into how computed target signatures may be used for target identification or verification. In real-world scenarios, an unknown target could be a variant of a particular target type having slightly different physical attributes. There could also be different configurations of equipment-accessory clutters on the targets. Since there is generally no a-priori information about an unknown target, and there is no knowledge of the target's variant type and the equipment clutter configuration on the target, this lack of information poses a major challenge to a target identification system, especially in compiling a database that can support a broad range of scenarios. Thus, a practical reference library of target images would be one that could provide general silhouette features or scatterers distributed in distinct spatial patterns as signatures of a particular target. The identification/verification process will then rely on human analysts to manually interpret the information from the captured unknown image and to correlate with the images in the reference library, extracting relevant target features to come up with an identification. Another conclusion emerges from this study is that in order to compile a good quality reference library, high-precision CAD models of the targets of interest must be acquired in order to generate reasonably accurate target features.

The electromagnetic modelling work presented in this work is currently being applied to support target characterization studies of marine targets (commercial ships) and small land targets (trucks) in collaborative projects with external research partners, e.g., NATO task groups. These studies will help to further develop the computational target signature capability for exploiting SAR imagery to extract target identification information. A collaborative project will be proposed to the CF Joint Imagery Centre to explore SAR image analysis techniques for finding and identifying various types of targets of interests, for example, ballistic missile launching platforms, ships and aircraft that are present at strategic locations of interest. The objective of the project is to help the CF to explore and develop enhanced capability for retrieving relevant target

information from SAR imagery data in support of mission planning, allowing the CF to be more effective in conducting their operations.

## References

---

- [1] R. van der Heiden, F. Groen, L. J. Van Ewijk, "Aircraft Recognition with Radar range profiles using a Synthetic Database", RTO Meeting Proceedings 40, "High resolution Techniques", NATO RTO-MP-40 AC/323(SET)TP/8, Neuilly-sur-Seine, Cedex, France, pp.57-1 to 57-8, November 1999.
- [2] D. Andersh, J. Moore, S. Kosanovich, D. Kapp, R. Bhalla, R. Kipp, T. Courtney, A. Nolan, F. German and J. Cook, "XPATCH 4: the next generation in high frequency electromagnetic modeling and simulation software", IEEE International Radar Conference 2000, pp.844-849, May 12-17, 2000, Alexandria VA USA.
- [3] A. L. Drozd, "Progress on the development of standards and recommended practices for CEM computer modeling and code validation", IEEE International Symposium on Electromagnetic Compatibility 2003, pp.313-316, vol.1, August 18-22, 2003.
- [4] A. L. Drozd, "Selected methods for validating computational electromagnetic modeling techniques", IEEE International Symposium on Electromagnetic Compatibility, pp.301-306, vol.1, August 8-12, 2005.
- [5] J. F. dawson, M. P. Robinson and T. Konefal, "Computational electromagnetic model (CEM) validation against measured and calculated results", IEE Seminar on Validation of Electromagnetics, pp.17-21, March 30, 2004.
- [6] A. Duffy, A. Martin, G. Antonini, A. Orlandi and C. Ritota, "The feature selective validation (FSV) method", IEEE International Symposium on Electromagnetic Compatibility 2005, pp.272-277, August 8-12, 2005
- [7] A. M. Raynal, R. Bhalla, H. Ling and V. J. Velton, "An algorithm for target validation using 3-D scattering features", Proceedings of SPIE, vol.6568, pp.1-8, May 2007.
- [8] J. G. Gallagher, "FACETS Prediction Code", RTO Meeting Proceedings 06, "Non-cooperative Air Target Identification using Radar", NATO RTO-MP-6 AC/323(SCI)TP/2, Neuilly-sur-Seine, Cedex, France, pp. 25-1 to 25-7, April 1998.
- [9] S. Wong, "Validation of the electromagnetic code FACETS for numerical simulation of radar target images", Technical Memorandum, DRDC Ottawa TM 2009-275, December 2009.
- [10] A. O. Knapskog, "Characteristics of ships in harbour investigated in simultaneous images from TerraSAR-X and PicoSAR", IEEE Radar Conference 2010, pp.422-427, May 10-14, 2010 Washington DC USA.

This page intentionally left blank.

<b>DOCUMENT CONTROL DATA</b>		
(Security classification of title, body of abstract and indexing annotation must be entered when the overall document is classified)		
<p>1. <b>ORIGINATOR</b> (The name and address of the organization preparing the document. Organizations for whom the document was prepared, e.g. Centre sponsoring a contractor's report, or tasking agency, are entered in section 8.)</p> <p><b>Defence R&amp;D Canada – Ottawa 3701 Carling Avenue Ottawa, Ontario K1A 0Z4</b></p>	<p>2. <b>SECURITY CLASSIFICATION</b> (Overall security classification of the document including special warning terms if applicable.)</p> <p><b>UNCLASSIFIED (NON-CONTROLLED GOODS) DMC A REVIEW: GCEC June 2010</b></p>	
<p>3. <b>TITLE</b> (The complete document title as indicated on the title page. Its classification should be indicated by the appropriate abbreviation (S, C or U) in parentheses after the title.)</p> <p><b>A comparative analysis of computed and measured SAR images of complex targets</b></p>		
<p>4. <b>AUTHORS</b> (last name, followed by initials – ranks, titles, etc. not to be used)</p> <p><b>S. Wong, N. Sandirasegaram, R. English, C. Liu, P. Vachon and J. Wolfe</b></p>		
<p>5. <b>DATE OF PUBLICATION</b> (Month and year of publication of document.)</p> <p><b>May 2012</b></p>	<p>6a. <b>NO. OF PAGES</b> (Total containing information, including Annexes, Appendices, etc.)</p> <p style="text-align: center;"><b>48</b></p>	<p>6b. <b>NO. OF REFS</b> (Total cited in document.)</p> <p style="text-align: center;"><b>10</b></p>
<p>7. <b>DESCRIPTIVE NOTES</b> (The category of the document, e.g. technical report, technical note or memorandum. If appropriate, enter the type of report, e.g. interim, progress, summary, annual or final. Give the inclusive dates when a specific reporting period is covered.)</p> <p><b>Technical Memorandum</b></p>		
<p>8. <b>SPONSORING ACTIVITY</b> (The name of the department project office or laboratory sponsoring the research and development – include address.)</p> <p><b>Defence R&amp;D Canada – Ottawa 3701 Carling Avenue Ottawa, Ontario K1A 0Z4</b></p>		
<p>9a. <b>PROJECT OR GRANT NO.</b> (If appropriate, the applicable research and development project or grant number under which the document was written. Please specify whether project or grant.)</p> <p><b>15eI05</b></p>	<p>9b. <b>CONTRACT NO.</b> (If appropriate, the applicable number under which the document was written.)</p>	
<p>10a. <b>ORIGINATOR'S DOCUMENT NUMBER</b> (The official document number by which the document is identified by the originating activity. This number must be unique to this document.)</p> <p><b>DRDC Ottawa TM 2012-016</b></p>	<p>10b. <b>OTHER DOCUMENT NO(s).</b> (Any other numbers which may be assigned this document either by the originator or by the sponsor.)</p>	
<p>11. <b>DOCUMENT AVAILABILITY</b> (Any limitations on further dissemination of the document, other than those imposed by security classification.)</p> <p><b>Unlimited</b></p>		
<p>12. <b>DOCUMENT ANNOUNCEMENT</b> (Any limitation to the bibliographic announcement of this document. This will normally correspond to the Document Availability (11). However, where further distribution (beyond the audience specified in (11) is possible, a wider announcement audience may be selected.)</p> <p><b>Unlimited</b></p>		

13. **ABSTRACT** (A brief and factual summary of the document. It may also appear elsewhere in the body of the document itself. It is highly desirable that the abstract of classified documents be unclassified. Each paragraph of the abstract shall begin with an indication of the security classification of the information in the paragraph (unless the document itself is unclassified) represented as (S), (C), (R), or (U). It is not necessary to include here abstracts in both official languages unless the text is bilingual.)

Computational radar target signature generation is considered as an integral component of a future target recognition system. It provides a comprehensive reference library database for target identification of a wide variety of targets, for example, aircraft, marine vessels and ground vehicles. Compiling an operational library will require an electromagnetic code that is capable of generating reliable and robust radar target signatures. Presently, computational electromagnetic modelling technology is not yet mature sufficiently to provide such a capability. To assess the quality of the computed target signatures from what is available with current technology, SAR (Synthetic Aperture Radar) images of complex targets generated by electromagnetic modelling computation are compared against measured SAR data of real targets.

An armoured personnel carrier, a self-propelled howitzer, a naval warship and a sea-going ferry are used as targets in the investigation. The commercial electromagnetic modelling code FACETS (Frequency Asymptotic Code for Electromagnetic Target Scattering) is used for generating the SAR images. CAD (Computer-Aided Design) models of targets of interest are used as inputs to the modelling code. Measured SAR images of corresponding targets from the public release MSTAR (Moving and Stationary Target Acquisition and Recognition) datasets and from the RadarSat2 SAR imagery archive are used to compare against the computed images. The objective is to analyze and characterize the computed image of complex targets; this facilitates a better understanding of the computational target signature generation problem.

14. **KEYWORDS, DESCRIPTORS or IDENTIFIERS** (Technically meaningful terms or short phrases that characterize a document and could be helpful in cataloguing the document. They should be selected so that no security classification is required. Identifiers, such as equipment model designation, trade name, military project code name, geographic location may also be included. If possible keywords should be selected from a published thesaurus, e.g. Thesaurus of Engineering and Scientific Terms (TEST) and that thesaurus identified. If it is not possible to select indexing terms which are Unclassified, the classification of each should be indicated as with the title.)

synthetic target signature generation, Synthetic Aperture Radar, computational electromagnetic modelling, target identification, target verification



## **Defence R&D Canada**

Canada's leader in Defence  
and National Security  
Science and Technology

## **R & D pour la défense Canada**

Chef de file au Canada en matière  
de science et de technologie pour  
la défense et la sécurité nationale



[www.drdc-rddc.gc.ca](http://www.drdc-rddc.gc.ca)